arXiv:1604.00929v1 [math.NA] 4 Apr 2016

MATHEMATICS OF COMPUTATION
Volume 00, Number 0, Pages 000–000
S 0025-5718(XX)0000-0

APPLICATION OF MODAL FILTERING TO A SPECTRAL DIFFERENCE METHOD

JAN GLAUBITZ, PHILIPP ÖFFNER, AND THOMAS SONAR

Abstract. We adapt the spectral viscosity (SV) formulation implemented as a modal filter to a Spectral Difference Method (SD) solving hyperbolic conservation laws. In the SD Method we use selections of different orthogonal polynomials (APK polynomials). Furthermore we obtain new error bounds for filtered APK extensions of smooth functions. We demonstrate that the modal filter also depends on the chosen polynomial basis in the SD Method. Spectral filtering stabilizes the scheme and leaves weaker oscillations. Hence, the selection of the family of orthogonal polynomials on triangles and their specific modal filter possesses a positive influence on the stability and accuracy of the SD Method. In the second part, we initiate a stability analysis for a linear scalar test case with periodic initial condition to find the best selection of APK polynomials and their specific modal filter. To the best of our knowledge, this work is the first that gives a stability analysis for a scheme with spectral filtering. Finally, we demonstrate the influence of the underlying basis of APK polynomials in a well-known test case.

1. Introduction

In the field of Computational Fluid Dynamics (CFD), low-order methods are generally robust and reliable and therefore employed in practical calculations. The main advantage of high-order methods towards low-order ones is the possibility of considerably more accurate solutions with the same computing cost, but unfortunately they are less robust and more complicated. In recent years many researchers focus on this topic. There has been a surge of research activities to improve and refine high-order methods as well as to develop new ones with more favorable properties. The Spectral Difference (SD) Method for simplex cells was first presented by Liu et al. [24], and later extended by Wang et al. [46, 37]. For one-dimensional, two-dimensional quadrilateral and three-dimensional hexahedral grids, the classical SD Method is identical to the multi-domain staggered grid spectral element method proposed by Kopriva et al. [22, 23]. Further contributions can be found inter alia in [14, 27, 40]. There are many publications that show that the classical SD Method is closely related to the Discontinuous Galerkin (DG) Method and Spectral Volume Method (or the same), see [1, 15, 49, 45, 39, 16, 18] for example. Depending on how the degrees of freedom (DOFs) are chosen, various method implementations have different numerical properties and efficiencies. But all of them have in common that

Received by the editor April 1, 2016.
2010 *Mathematics Subject Classification.* Primary 65M12,65M70; Secondary 42C10.
Key words and phrases. hyperbolic conservation laws, high order methods, Spectral Difference Method, orthogonal polynomials, modal filtering.

©XXXX American Mathematical Society

they use piecewise continuous functions as approximation space for solutions. Here, we apply the classical orthogonal polynomials on triangles in a Spectral Difference Method and focus on filtering techniques. We don't use the nowadays more common Flux Reconstruction (FR) or Correction Procedure via Reconstruction (CPR) methods, because we only want to investigate the pure influence of the orthogonal polynomials and their natural filters. In the FR/CPR approach, a correction term[1] is applied which works at the interface and rectify the calculation in in every step, for details see [35, 15, 42, 17, 43] and references therein. Furthermore, the SD Method on triangular grids is not stable, i.e. numerical solutions migth exceed all boundaries where they shouldn't. This allows us to oberve the influence of filter techniques and how they enable us to milder such instabilities of the scheme. The SD Method combines the basic ideas of spectral methods and finite differences. It directly reconstructs a flux polynomial based on fluxes on a given nodal set called flux points. Then the derivatives of the flux polynomial are used to update the solutions at the solution points. This approach prevents the use of quadrature rules like in a normal DG or Spectral Volume ansatz[2]. However, the SD Method has stability issues especially for high orders or if discontinuities arise in the solution. The root of the instability is that the nonlinear flux function is represented by an insufficient amount of points. This introduces aliasing errors [20]. By increasing the dissipation we are able to mask such an aliasing problem. We apply the same approach like in spectral methods and use spectral viscosity to stabilize the calculation, see [26, 38]. As suggested in [25], the spectral viscosity can be carried out within the spectral filtering framework, resulting in an efficient computational implementation. The Spectral Viscosity Method (SV) can be seen as a spectral method, but at each time step the numerical solution is filtered by an exponential filter which depends on the chosen set of orthogonal polynomials.
Meister et al. [28] apply the Proriol-Koornwinder-Dubiner (PKD) polynomials in a DG Method and derive a relation between a modal filter for DG Methods on unstructured triangulation grids and the introduction of spectral viscosity to the scheme. The basic idea is to add a high order viscosity term, which is based on the Sturm-Liouville Operator of the polynomials to the equation.
In this article, we consider the Spectral Difference Method as described in [48], but we extend it by the general classical orthogonal polynomials on triangles (APK polynomials)[3] and their specific modal filters. With the differential operator of the APK polynomials, we show analogous to [28] the close relation between SV and spectral filtering in the SD Method.
In a theoretical framework we prove some new upper bounds for the filtered APK expansion of smooth functions. Here, we generalize the theoretical results from [28], where only the properties of the filtered PKD expansion were analyzed. Our viscosity term depends on the differential operator of the chosen polynomial set and so the exponential filter as well. Therefore the selection of the orthogonal polynomials and their natural filter have a positive impact on the stability and accuracy

[1]With appropriate choices of correction terms, the FR framework recovers specific DG, SD, as well as spectral volume schemes.

[2]There exists also quadrature-free implementations of DG, see for example [2].

[3]The PKD or Dubiner polynomials are only one specific family of these polynomials.

of the method. By starting a stability analysis as presented in [15, 40] we get a better understanding of the influence of the orthogonal polynomials and their specific filters.

This paper is organized as follows:
In section 2 we will define these considered polynomials and review some properties. We will repeat the main ideas on the Spectral Difference Method and explain our implementation in the next section. High order filters as the SV Method as stabilizing technique are introduced in section 4. Also, we prove an error bound for the filtered APK expansion of smooth functions and transfer the SV modification to our SD Method. In section 5 we start with the stability analysis for our SD Method. A numerical experiment is presented before a conclusion and an outlook for future work finishes this paper.

2. Appell-Proriol-Koornwinder polynomials and their properties

In this section we introduce the orthogonal polynomials under observation. We call the family of classical orthogonal polynomials on triangles Appell-Proriol-Koornwinder polynomials (APK polynomials). In [31] the authors prove spectral convergence for the APK series. Their result gives us the theoretical foundation to use these polynomials in a spectral method.
Let $P_n^{\alpha,\beta}(x)$ be the n-th Jacobi polynomial, $\mathbb{T} := \{(x,y) \in \mathbb{R}^2 | x \geq 0, y \geq 0, x+y \leq 1\}$ be the unit triangle and $h(x,y) := x^{\alpha-1}y^{\beta-1}(1-x-y)^{\gamma-\alpha-\beta}$ ($\alpha,\beta,\gamma \in \mathbb{N}, \gamma > \alpha+\beta-1$ and $\mathbb{N} = \{1,2,\cdots\}$) be the weight function, given in this domain. For the sake of brevity, we introduce $p = \gamma-\alpha-\beta$ and $a_l = p+\beta+2l$.
Note that we only use $\alpha,\beta,\gamma \in \mathbb{N}$ for simplicity. In principle, $\alpha,\beta,\gamma \in \mathbb{R}_0^+$ is possible.

Definition 2.1. The polynomials $A_{m,l}(x,y)$, $m,l \in \mathbb{N}_0$, defined as

$$A_{m,l}(x,y) := P_m^{\alpha-1,a_l}(1-2x)P_l^{p,\beta-1}\left(\frac{2y}{1-x}-1\right)(1-x)^l \tag{2.1}$$

on $\mathbb{T}$ are called *Appell-Proriol-Koornwinder polynomials* (APK polynomials).
If the triangle $\widetilde{\mathbb{T}} := \{(x,y) \in \mathbb{R}^2 | x \geq -1, y \geq -1, x+y \leq 0\}$ is used instead, then (2.1) transforms to

$$\widetilde{A}_{m,k}(x,y) = P_m^{\alpha-1,2l+\gamma-\alpha}(-x)P_l^{\gamma-\alpha-\beta,\beta-1}\left(\frac{2(y+1)}{1-x}-1\right)\left(\frac{1-x}{2}\right)^l.$$

The special case $\alpha = \beta = 1$ and $\gamma = 2$ is called Proriol-Koornwinder-Dubiner polynomial (PKD polynomials)(see [6, 19]) .

These are the classical orthogonal polynomials on triangles. Details of their properties can be found in [7, 21, 36]. We start with the definition of the function spaces and norms we are dealing with. Then we summarize some of the properties of APK polynomials and give a couple of estimates, which are needed in the sequel. The detailed proofs of these estimates can be found in [31].

Definition 2.2. Let $h(x,y)$ be the weight function on the triangle $\mathbb{T}$. We denote by $\mathbb{L}^2(\mathbb{T},h)$ the Hilbert space with the inner product

$$(u,v) := \int_{\mathbb{T}} h(x,y)u(x,y)v(x,y)dxdy$$

which induces the weighted norm

$$||u||_{\mathbb{L}^2(\mathbb{T},h)} := \left(\int_{\mathbb{T}} h(x,y)|u(x,y)|^2 dxdy\right)^{\frac{1}{2}}.$$

We introduce by $H^m(\mathbb{T},h)$ a *weighted Sobolev space*. Precisely we set

$$H^m(\mathbb{T},h) := \{v \in \mathbb{L}^2(\mathbb{T},h) : \text{for each non-negative multi-index } \sigma \text{ with } |\sigma| \leq m, \text{ the distributional derivative } D^\sigma v \text{ belongs to } \mathbb{L}^2(\mathbb{T},h)\}.$$

The space is endowed with the norm

$$||v||_{H^m(\mathbb{T},h)} := \left(\sum_{|\sigma|\leq m} ||D^\sigma v||^2_{\mathbb{L}^2(\mathbb{T},h)}\right)^{\frac{1}{2}}.$$

The APK polynomials are characterized by the integers m and l as can be seen in the definition. The degree of an APK polynomial then is $N := m + l$. First of all we give the statement on the orthogonality of these polynomials with respect to the weight function h.

Lemma 2.3. *The APK polynomials $A_{m,l}$ are orthogonal on the triangle $\mathbb{T}$ with respect to the inner product*

$$(A_{m,l}, A_{n,s}) = \delta_{m,n}\delta_{l,s}\frac{1}{(2l+\gamma-\alpha)(2(m+l)+\gamma)\kappa^2_{l,m}}$$

with $\kappa_{l,m} := \sqrt{\frac{(l+\beta)_p m(m+a_l)_\alpha}{(l+1)_p(m)_\alpha(m+a_l)}}$ and

$$(\xi)_0 = 1, (\xi)_j = \prod_{i=0}^{j}(\xi+i-1) \text{ for } j \in \mathbb{N}$$

is the usual Pochhammer symbol.

Proof. See [36, Chapter X. p.288ff]. □

Another important property of the APK polynomials can be found in the fact that they are solutions to the eigenvalue problem

$$DA_{m,l} = \lambda_{m,l}A_{m,l} \tag{2.2}$$

where the differential operator D is given by

$$(x^2-x)\frac{\partial^2}{\partial x^2} + 2xy\frac{\partial^2}{\partial x\partial y} + (y^2-y)\frac{\partial^2}{\partial y^2} + [(\gamma+1)x-\alpha]\frac{\partial}{\partial x} + [(\gamma+1)y-\beta]\frac{\partial}{\partial y},$$

and the eigenvalue $\lambda_{m,l} = (m+l)(m+l+\gamma)$, see [7, p.46]. Note that this eigenvalue equation is *not* a Sturm-Liouville problem and also that the differential operator is not self-adjoint for all choices of α, β, γ. It is only self-adjoint in case of $\alpha = \beta = 1$ and $\gamma = 2$. But in fact, the operator is, what is called, *potentially self-adjoint* in $\mathring{T}$, see [36, p.136]. Hence there exists a positive C^2- function g, $(x,y) \mapsto g(x,y)$, so that gD is self-adjoint in $\mathring{\mathbb{T}}$. This will be important in section 4, when we use the differential operator in the viscosity term. In the following lemmas we summarize the estimates which will be needed in the proof of Theorem 4.3. The proofs can be found in [31].

Lemma 2.4. *The following norm estimate holds for APK polynomials,*

$$\frac{1}{||A_{m,l}||_{L^2(\mathbb{T},h)}} \leq 2(m+l+\gamma)\kappa_{l,m} \tag{2.3}$$

with $\kappa_{l,m}$ *as in* Lemma 2.3.

Furthermore let $(x,y) \in \mathring{\mathbb{T}}$. *For all* $l,m \in \mathbb{N}_0$ *the following estimate holds,*

$$|A_{m,l}(x,y)| \leq \frac{\tilde{D}(x,y)}{(2l+\beta+p)^{\frac{1}{4}}(2(m+l)+\gamma)^{\frac{1}{4}}\kappa_{l,m}}, \tag{2.4}$$

where

$$\tilde{D}(x,y) = \frac{D}{2(1-x-y)^{\frac{p}{2}+\frac{1}{4}}y^{\frac{1}{4}+\frac{\beta-1}{2}}x^{\frac{1}{4}+\frac{\alpha-1}{2}}(1-x)^{\frac{1}{4}}}$$

and $D < 144$ *is a positive constant. On the edge* $[0,y]$ *with* $y \in [0,1]$ *we have*

$$|A_{m,l}(0,y)| \leq \left(\binom{m+\alpha-1}{m} \cdot \max\left\{\binom{l+p}{l}, \binom{l+\beta-1}{l}\right\}\right). \tag{2.5}$$

On the edges $[x,1-x]$ *and* $[x,0]$ *the following holds*

$$\begin{aligned} |A_{m,l}(x,0)| \leq & \frac{C}{(2(m+l)+\gamma)^{\frac{1}{4}}(x)^{\frac{1}{4}+\frac{\alpha-1}{2}}((1-x))^{\frac{1}{4}+\frac{\gamma-\alpha}{2}}\sqrt{2}} \cdot \\ & \cdot \left(\frac{(m)_\alpha(m+a_l)}{(m+a_l)_\alpha m}\right)^{\frac{1}{2}} \binom{l+\beta-1}{l} \end{aligned} \tag{2.6}$$

and

$$\begin{aligned} |A_{m,l}(x,1-x)| \leq & \frac{C}{(2(m+l)+\gamma)^{\frac{1}{4}}(x)^{\frac{1}{4}+\frac{\alpha-1}{2}}((1-x))^{\frac{1}{4}+\frac{\gamma-\alpha}{2}}\sqrt{2}} \cdot \\ & \cdot \left(\frac{(m)_\alpha(m+a_l)}{(m+a_l)_\alpha m}\right)^{\frac{1}{2}} \binom{l+p}{l} \end{aligned} \tag{2.7}$$

valid for all $x \in (0,1)$ *with a positive constant* $C < 12$. *The value of* $A_{m,l}(1,0)$ *is*

$$|A_{m,l}(1,0)| = \begin{cases} \binom{m+\gamma-\alpha}{m} & \text{if } l = 0 \\ 0 & \text{else} \end{cases}. \tag{2.8}$$

Remark 2.5. We note that $C < 12$ is only known at the moment (see [12]).

The last estimates, which we will apply in Theorem 4.3, are direct from the main Theorem of [31]. We need these estimations, when analyzing the approximation properties of the filtered APK expansion of smooth functions.

Theorem 2.6. *Let* u *be a function in the space* $H^{2k}(\mathbb{T},h) \cap C(\mathbb{T}), k \in \mathbb{N}$ *where* $h(x,y) = x^{\alpha-1}y^{\beta-1}(1-x-y)^p$ *the weight with* $\alpha,\beta \in \mathbb{N}$ *and* $p \in \mathbb{N}_0$. *The APK expansion of* u *is given by*

$$P_N u(x,y) = \sum_{\substack{l+m \leq N \\ l,m \in \mathbb{N}_0}} \tilde{u}_{m,l} A_{m,l}(x,y); \quad \tilde{u}_{m,l} = \frac{(u; A_{m,l})_{\mathbb{L}^2(\mathbb{T},h)}}{(A_{m,l}; A_{m,l})_{\mathbb{L}^2(\mathbb{T},h)}}. \tag{2.9}$$

The following estimates hold:

$$(A_{m,l}; A_{m,l})^{\frac{1}{2}}_{\mathbb{L}^2(\mathbb{T},h)} \cdot |\tilde{u}_{m,l}| = \mathcal{O}(\lambda_{m,l}^{-k}), (m+l) \to \infty, \tag{2.10}$$

$$||u - P_N u||_{\mathbb{L}^2(\mathbb{T},h)} = \mathcal{O}(N^{-2k}), N \to \infty. \tag{2.11}$$

For the pointwise estimations following hold:

(a) *if* $\beta - 1 < p$ *and* $1 + \frac{p+\beta}{2} \leq \frac{3}{4} + \frac{3}{4}\alpha + \frac{p}{2} < k$ *:*

$$|u(x,y) - P_N u(x,y)| = \mathcal{O}(N^{-2k+\frac{3}{2}\alpha+p+\frac{1}{2}}), \quad \forall (x,y) \in \mathbb{T}, \tag{2.12}$$

(b) *if* $\beta - 1 < p$ *and* $\frac{3}{4} + \frac{3}{4}\alpha + \frac{p}{2} \leq 1 + \frac{p+\beta}{2} < k$*:*

$$|u(x,y) - P_N u(x,y)| = \mathcal{O}(N^{-2k+p+\beta+\frac{3}{2}}), \quad \forall (x,y) \in \mathbb{T}, \tag{2.13}$$

(c) *if* $p \leq \beta - 1$ *and* $1 + \frac{p+\beta}{2} \leq \frac{1}{4} + \frac{3}{4}\alpha + \frac{\beta}{2} < k$*:*

$$|u(x,y) - P_N u(x,y)| = \mathcal{O}(N^{-2k+\frac{3}{2}\alpha+\beta-\frac{1}{2}}), \quad \forall (x,y) \in \mathbb{T}, \tag{2.14}$$

(d) *if* $p \leq \beta - 1$ *and* $\frac{1}{4} + \frac{3}{4}\alpha + \frac{\beta}{2} \leq 1 + \frac{p+\beta}{2} < k$*:*

$$|u(x,y) - P_N u(x,y)| = \mathcal{O}(N^{-2k+p+\beta+\frac{3}{2}}), \quad \forall (x,y) \in \mathbb{T}. \tag{2.15}$$

3. An extended Spectral Difference Method

In this paper we consider two-dimensional hyperbolic conservation laws of the form

$$\frac{\partial}{\partial t}\boldsymbol{u}(\boldsymbol{x},t) = -\nabla_{\boldsymbol{x}} F(\boldsymbol{u}(\boldsymbol{x},t)), \quad (\boldsymbol{x},t) \in \Omega \times \mathbb{R}_0^+, \tag{3.1}$$

where $\Omega \subset \mathbb{R}^2$ is an open polygonal domain and $\boldsymbol{u}(\boldsymbol{x},t) \in \mathbb{R}^n$. Furthermore, initial conditions $\boldsymbol{u}(\boldsymbol{x},0) = \boldsymbol{u}_0(\boldsymbol{x})$ and appropriate boundary conditions are assumed to be given.

Hence, let $\mathcal{T}_h$ be a conforming triangulation of the closure $\overline{\Omega}$ of the computational domain and let $\mathbb{P}^h$ be the piecewise polynomial space defined by $\mathbb{P}^h = \{v_h \in L^\infty(\Omega) \mid v_h|_{\tau_i} \in \mathcal{P}^N(\tau_i), \ \ \forall \tau_i \in \mathcal{T}_h\}$, where $\mathcal{P}^N(\tau_i)$ denotes the space of all polynomials on τ_i of degree less or equal than N.

The classical Spectral Difference Method, which has been proposed by Liu [24] in 2006, can be seen as a FR or collocation method. The basic idea of this method is to discretize the right hand side of the underlaying conservation law (3.1) at certain solution points $\mathbf{x_j}$ in each cell. Then, the resulting ODEs (in t) at each $\mathbf{x}_j$ can be solved by an arbitrary explicit time-stepping scheme. Here we used the 4-th order low storage Runge-Kutta scheme defined by Carpenter and Kennedy, see [5]. We say that a scheme is of *order* $N+1$, when it is exact for $\boldsymbol{u} \in \left[\mathcal{P}^N\right]^n$. Since the derivate of the flux F is applied to update $\boldsymbol{u}$, one needs to be exact for $F \in \left[\mathcal{P}^{N+1}\right]^{n\times 2}$. We approximate the flux F in each element τ_i of our triangulation $\mathcal{T}_h$ using the basis polynomials ϕ_k in the following way

$$\begin{pmatrix} F_1(\boldsymbol{x},t) \\ F_2(\boldsymbol{x},t) \end{pmatrix} = \sum_{k=1}^{K_F} \begin{pmatrix} \hat{F}_{k,1}(t) \\ \hat{F}_{k,2}(t) \end{pmatrix} \phi_k(\boldsymbol{x}). \tag{3.2}$$

The classical approach uses Lagrange polynomials L_k with corresponding coefficients $\hat{F}_{k,\nu}(t) = F_\nu(\mathbf{x}_k, t)$ for $\nu = 1, 2$, where $\mathbf{x}_k$ are chosen flux points. If we want to achieve a method of order $N+1$, we need the reconstruction of the solution $\boldsymbol{u}$ to lie in $\left[\mathcal{P}^N\right]^n$ and the reconstruction of the flux F to lie in $\left[\mathcal{P}^{N+1}\right]^{n\times 2}$. Hence we need $K_s := \frac{(N+1)(N+2)}{2}$ solution points $\mathbf{x_j}$ and $K_F := \frac{(N+2)(N+3)}{2}$ flux points $\mathbf{x_k}$. That means points where the flux value is computed. Here we apply the classic orthogonal polynomials on triangles $\phi_k = A_{m,l}$ (in lexicographic order k). In order to adapt the polynomial basis ϕ_k to every triangular cell τ_i, we introduce an

orientation-preserving affine transformation T_i which maps an arbitrary triangle τ_i to the standard triangle $\mathbb{T}$ of the orthogonal basis ϕ_k, see Figure 1. By linearity of

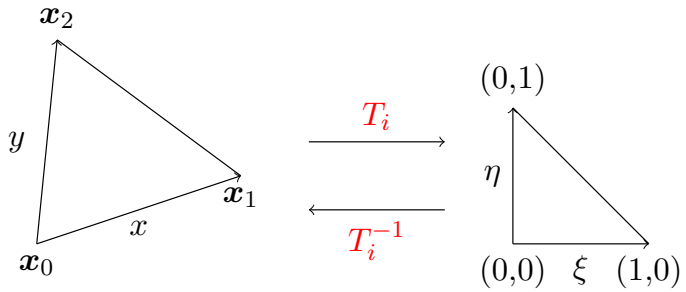

FIGURE 1. transformation of an arbitrary triangle to the standard element

the differential operator, inserting (3.2) into (3.1) leads to

$$\boldsymbol{u}_t(\boldsymbol{x},t) = -\sum_{k=1}^{K_F} \begin{pmatrix} \hat{F}_{k,1}(t) \\ \hat{F}_{k,2}(t) \end{pmatrix} \cdot \nabla_{\boldsymbol{x}} \phi_k(T_i(\boldsymbol{x})).$$

Applying the transformation and the chain rule to

$$\nabla_{\boldsymbol{x}} \phi_k(T_i(\boldsymbol{x})) = J_{T_i} \nabla_{\boldsymbol{\xi}} \phi_k(T_i(\boldsymbol{x})),$$

finally leads to the universal update scheme

$$\boldsymbol{u}_t(\boldsymbol{x},t) = -\sum_{k=1}^{K_F} \begin{pmatrix} \hat{F}_{k,1}(t) \\ \hat{F}_{k,2}(t) \end{pmatrix} \cdot J_{T_i} \nabla_{\boldsymbol{\xi}} \phi_k(T_i(\boldsymbol{x})). \tag{3.3}$$

where for each cell only the Jacobian J_{T_i} has to be stored. For the stability analysis in section 5 we will derive benefit from the following matrix representation of (3.3). If we denote the vector $\big(\boldsymbol{u}_t(\mathbf{x}_j,t)\big)_j$ at the K_s solution points $\mathbf{x}_j$ by $\frac{\mathrm{d}\mathbf{u}^s}{\mathrm{d}t}(t)$ and J_{T_i} by $\begin{pmatrix} \xi_x & \xi_y \\ \eta_x & \eta_y \end{pmatrix}$, the universal update scheme reads

$$\begin{aligned} \frac{\mathrm{d}\mathbf{u}^s}{\mathrm{d}t}(t) = &- \Big(\sum_{k=1}^{K_F} \hat{F}_{k,1}(t) \big[\xi_x \partial_\xi \phi_k(T_i(\mathbf{x}_j)) + \xi_y \partial_\eta \phi_k(T_i(\mathbf{x}_j)) \big] \Big)_j \\ &- \Big(\sum_{k=1}^{K_F} \hat{F}_{k,2}(t) \big[\eta_x \partial_\xi \phi_k(T_i(\mathbf{x}_j)) + \eta_y \partial_\eta \phi_k(T_i(\mathbf{x}_j)) \big] \Big)_j \\ = &- \xi_x D_\xi \hat{\mathbf{F}}_1(t) - \xi_y D_\eta \hat{\mathbf{F}}_1(t) - \eta_x D_\xi \hat{\mathbf{F}}_2(t) - \eta_y D_\eta \hat{\mathbf{F}}_2(t) \end{aligned} \tag{3.4}$$

with

$$\begin{aligned} D_\xi &= \big(\partial_\xi \phi_k(T_i(\mathbf{x}_j))\big)_{j,k}\,, \ \hat{\mathbf{F}}_1(t) = \big(\hat{F}_{k,1}(t)\big)_k \ \text{ and} \\ D_\eta &= \big(\partial_\eta \phi_k(T_i(\mathbf{x}_j))\big)_{j,k}\,, \ \hat{\mathbf{F}}_2(t) = \big(\hat{F}_{k,2}(t)\big)_k. \end{aligned} \tag{3.5}$$

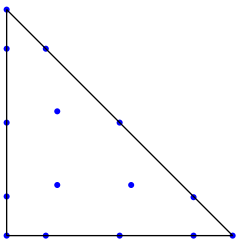

Lobatto points, order 4

In spite of the Lagrange reconstruction approach where the flux coefficients are directly known we have to compute $\hat{F}_{k,\nu}(t)$, in every time step. We choose an interpolation approach, i.e. we interpolate the values of the flux function at certain flux points $\{\mathbf{x}_k\}$ from the given flux F, which will be specified later on. The nodal set $\{\mathbf{x}_k\}$ is chosen as the set of two dimensional Lobatto points on a triangle, see Figure 3, proposed by Blyth and Pozrikidis [4] since they are easy to implement and have good interpolation properties, as for instance a low condition number.

The condition number of the Vandermonde matrix $\mathcal{V}$ in the interpolation approach depends on the parameters α, β and γ of the APK polynomials, see Table 1. The numbers in the braces describe the parameters (α, β, γ) of the APK-polynomials. We realize that Lagrange polynomials lead to completely bad conditioned basis compared to any of the considered APK families. Regarding this, one should note that the coefficients of the Lagrange reconstruction are directly given by the values of the flux at the flux points. This values however are obtained from the values of the flux at the solution points by Lagrange interpolation. Additional numerical errors might arise.

N	2	3	4	5	6	7	8	9	10
Lagr. poly.	24	270	2023	10^4	10^5	$7 \cdot 10^5$	$5 \cdot 10^6$	$3 \cdot 10^7$	$2 \cdot 10^8$
$(0.1, 0.1, 0.2)$	72	23	103	162	305	315	429	577	681
$(0.5, 0.5, 1)$	12	17	30	42	52	71	82	100	121
$(1, 1, 2)$	12	20	39	53	71	94	121	151	196
$(1, 1, 6)$	29	117	391	973	2365	4484	8008	10^4	$2 \cdot 10^4$
$(2, 2, 5)$	17	44	96	161	244	450	662	853	1341
$(3, 3, 20)$	28	131	416	929	2310	4711	10^4	$2 \cdot 10^4$	$3 \cdot 10^4$
$(10, 10, 20)$	306	2307	$2 \cdot 10^4$	$8 \cdot 10^4$	$4 \cdot 10^5$	$2 \cdot 10^6$	$8 \cdot 10^6$	$2 \cdot 10^7$	$8 \cdot 10^7$
$(1, 2, 3)$	11	33	66	99	147	209	295	409	532
$(2, 1, 3)$	17	34	66	123	178	243	388	446	570

TABLE 1. condition numbers κ_N

Additionally, enough flux points lie on the edges of an element to ensure global conservation [47], which is then realized by replacing the original flux F at flux points $\mathbf{x}_k$ at the edges by a numerical flux F^{num} whose normal component is computed from a numerical flux function H, i.e. $F_k^{num} \cdot \mathbf{n} = H(\boldsymbol{u}_-(\mathbf{x}_k, t), \boldsymbol{u}_+(\mathbf{x_k}, t), \mathbf{n})$. The whole flux is used in the scheme, so that one needs a second condition to determine the numerical flux. As in [44], we enforce F^{num} to maintain the same tangential component as the original flux, i.e. $F_k^{num} \cdot \mathbf{t} = F(\boldsymbol{u}(\mathbf{x}_k, t)) \cdot \mathbf{t}$, which uniquely defines the numerical flux $F_k^{num} = (F_{k,1}^{num}, F_{k,2}^{num})^T$ at each edge point $\mathbf{x}_k$. Now, the coefficients $\hat{F}_{k,\nu}(t)$ in equation (3.3) can be computed by solving the system of equation $\mathbf{F}_\nu(t) = \mathcal{V} \cdot \hat{\mathbf{F}}_\nu(t)$ for each component $\nu = 1, 2$, where $\hat{\mathbf{F}}_\nu = \left(\hat{F}_{k,\nu}(t)\right)_k$, $\mathcal{V} = (\phi_k(\mathbf{x_j}))_{j,k}$ is the Vandermonde matrix and $\hat{\mathbf{F}}_\nu(t) = (F_{k,\nu})_k$

is given by

$$F_{k,\nu} = \begin{cases} F_\nu(\boldsymbol{u}(\mathbf{x}_k, t)), & \text{if } \mathbf{x}_k \in \mathring{\tau}_i \\ F_{k,\nu}^{num}, & \text{if } \mathbf{x}_k \in \partial\tau_i. \end{cases} \tag{3.6}$$

If we apply this to (3.4) the universal update scheme reads

$$\frac{\mathrm{d}\mathbf{u}^s}{\mathrm{d}t}(t) = -(\xi_x D_\xi + \xi_y D_\eta)\mathcal{V}^{-1}\mathbf{F}_1(t) - (\eta_x D_\xi + \eta_y D_\eta)\mathcal{V}^{-1}\mathbf{F}_2(t) \tag{3.7}$$

in a matrix representation. In section 5 we will use this result to obtain the form

$$\frac{\mathrm{d}\mathbf{u}^s}{\mathrm{d}t}(t) = S\mathbf{u}^s(t)$$

with a matrix S for a suitable test case. In the numerical examples in section 6 we will use the **Godunov flux**

$$H(u_-, u_+, \mathbf{n}) = \begin{cases} \min\limits_{u_- \le u \le u_+} F(u)\cdot\mathbf{n}, & \text{if } u_- \le u_+, \\ \max\limits_{u_+ \le u \le u_-} F(u)\cdot\mathbf{n}, & \text{else,} \end{cases}$$

in the scalar case for the numerical flux function. The Godunov flux is an **Upwind flux**. For the linear transport equation we obtain the numerical flux

$$H(u_-, u_+, \mathbf{n}) = \begin{cases} (\mathbf{a}\cdot\mathbf{n})u_-, & (\mathbf{a}\cdot\mathbf{n}) \ge 0, \\ (\mathbf{a}\cdot\mathbf{n})u_+, & (\mathbf{a}\cdot\mathbf{n}) < 0. \end{cases}$$

We will apply this numerical flux function in the stability analysis in section 5 as well.

We use the same method as displayed in [30]. For a more detailed explanation of the Spectral Difference Method and the extension we advise [47].

4. The filtering process

In the conservation law, discontinuities may arise in the solution. Using a series expansion to approximate the solution leads to spurious oscillations in the vicinity of discontinuities (called Gibbs phenomenon). The oscillations occur in the approximated solution because the high coefficients of the series expansion turns slowly to zero, see [10, 11].

The aliasing error effects stability problems in the SD Method. The root of the instabilities is that the nonlinear flux function is represented by an insufficient amount of points. This introduces aliasing errors. These stability problems display especially near the oscillations. The amplitudes increase in time exceeding the error expected from the pure Gibbs phenomenon, see section 6. A higher inherent dissipation is able to mask such an aliasing problem. By adding spectral viscosity to the equation we increase the dissipation.

To remedy the Gibbs' effect, different approaches can be found in the literature [8, 9, 11, 41]. A common approach is to use a modal filter, which appeals directly on the high-order coefficients of the series expansion. While multiplying a filter function to the high Fourier coefficients, the series loses their approximation properties. We prove new error bounds for the filtered APK series expansion of smooth function. We generalize the results of [28] to all series expansion with classic orthogonal polynomials on triangles. Global filtering in each cell degrades the order of accuracy, see [28]. Therefore we apply a well-known jump indicator [34] and transfer the SV modification to the SD Method.

4.1. **Modal filters.** A modal filter appeals directly to the coefficients of the series expansion.

Definition 4.1. For an integer $p \geq 1$ we define a **filter** of order p as a real function $\sigma \in C^{p-1}([0,1])$ with the properties

$$\begin{aligned} \sigma(0) &= 1, \\ \sigma^{(k)}(0) &= 0, \qquad 1 \leq k \leq p-1. \end{aligned} \tag{4.1}$$

Additionally to the properties (4.1) many authors demand the following condition for a filter of order p:

$$\sigma^{(k)}(1) = 0 \qquad 0 \leq k \leq p-1, \tag{4.2}$$

compare [11, 41]. In [13], Hesthaven and Kirby require in addition $\sigma \in C^p([0,1])$. A very popular filter is the exponential filter

$$\sigma(\eta) = \exp(-\alpha \eta^p),$$

where the filter strength α yields $\exp(-\alpha)$ in the range of the machine accuracy. We already mentioned that there are various partial results for the approximation property of a filtered series expansion. Vandeven analyzes in [41] the filtered Fourier expansions of a piecewise smooth function. He proves the following error bound for the filtered partial sum

$$u_N^\sigma(x) = \sum_{|k| \leq N} \sigma\left(\frac{|k|}{N}\right) \hat{u}_k \mathsf{e}^{\mathsf{i}kx},$$

where $u_N(x) = \sum\limits_{|k| \leq N} \hat{u}_k \mathsf{e}^{\mathsf{i}kx}$ is the truncated Fourier expansions of $u(x)$.

Theorem 4.2. *Let σ be a filter of order p and $u : \mathbb{R} \to \mathbb{R}$ a piecewise 2π-periodic smooth function. The following estimations hold:*

1. *Let $u \in C^p(\mathbb{R})$. The error $|u(x) - u_N^\sigma(x)|$ is bounded by*

$$|u(x) - u_N^\sigma(x)| \leq C_1 \frac{1}{N^{p-\frac{1}{2}}}, \qquad x \in \mathbb{R}, \tag{4.3}$$

   where C_1 is a constant independent of x and N.
2. *If σ fulfills further the condition (4.2), u possesses one or more jump discontinuities and is continuous at $x \in \mathbb{R}$, then we have*

$$|u(x) - u_N^\sigma(x)| \leq C_2 \frac{1}{d(x)^{p-1} N^{p-1}},$$

   where $d(x)$ denotes the distance form x to the nearest discontinuity and C_2 is a constant independent of x and N.

Vandeven expanded his result to filtered Chebyshev series. Whereas, Kirby and Hesthaven investigate the approximation property of the filtered Legendre expansion for sufficiently smooth functions in [13]. They obtain a similar result to (4.3). [28] expands the investigation to two-dimensional basis functions (PKD polynomials) and also demonstrates a similar result to (4.3). Now we complete the investigation from [28], by proving an error bound for the filtered APK partial sum. The PKD polynomials are only one special case of the APK polynomials. Here we

prove the most general case and consider the filtered APK expansions for sufficiently smooth functions $u : \mathbb{T} \to \mathbb{R}$,

$$u_N^\sigma(x,y) = \sum_{l+m\leq N} \sigma\left(\frac{l+m}{N}\right) \tilde{u}_{m,l} A_{m,l}(x,y), \qquad N \geq 1,$$

with coefficients $\tilde{u}_{m,l}$ given by (2.9).

Theorem 4.3. *Let $u \in H^{2k}(\mathbb{T},h) \cap C(\mathbb{T}), k \in \mathbb{N}$, $h(x,y) = x^{\alpha-1}y^{\beta-1}(1-x-y)^p$ with $\alpha,\beta \in \mathbb{N}$ and $p \in \mathbb{N}_0$ and let σ be a modal filter of order $2k-1$, with the additional condition $\sigma \in C^{2k-1}([0,\varepsilon))$ in an interval $[0,\varepsilon) \subset [0,1]$, $\varepsilon > 0$. Furthermore let $k > \max\left\{ \frac{3}{4} + \frac{3}{4}\alpha + \frac{p}{2}, \frac{5}{4} + \frac{p+\beta}{2}, \frac{1}{4} + \frac{3}{4}\alpha + \frac{\beta}{2} \right\}$.*
Then we obtain the pointwise error bounds with constants $K_1 - K_6$:

(1) *If $(x,y) \in \mathring{\mathbb{T}}$, it is*

$$|u(x,y) - u_N^\sigma(x,y)| \leq K_1 \frac{1}{N^{2k-\frac{7}{4}}}.$$

(2) *On the left edge $[0,y]$ with $y \in [0,1]$ we obtain*

$$|u(0,y) - u_N^\sigma(0,y)| \leq \begin{cases} K_2 \frac{1}{N^{2k-\frac{3}{2}\alpha-p-\frac{1}{2}}}, & \text{for } p > \beta - 1, \\ K_3 \frac{1}{N^{2k-\frac{3}{2}\alpha-\beta+\frac{1}{2}}}, & \text{for } p \leq \beta - 1. \end{cases}$$

(3) *On the edge $[x,0]$ with $x \in (0,1)$ the error is*

$$|u(x,0) - u_N^\sigma(x,0)| \leq K_4 \frac{1}{N^{2k-\frac{3}{4}-\beta}}.$$

(4) *On the hypotenuse $[x,1-x]$ with $x \in (0,1)$ pertain*

$$|u(x,1-x) - u_N^\sigma(x,1-x)| \leq K_5 \frac{1}{N^{2k-\frac{7}{4}-p}}.$$

(5) *In the point $(1,0)$ we preserve*

$$|u(1,0) - u_N^\sigma(1,0)| \leq K_6 \frac{1}{N^{2k+\alpha-\gamma-\frac{3}{2}}},$$

Proof. We start the proof similar to [31, Theorem 3.1]. Let $m + l \neq 0$, then

$$(A_{m,l}; A_{m,l})_{\mathbb{L}^2(\mathbb{T},h)} \cdot |\tilde{u}_{m,l}| = (u; A_{m,l})_{\mathbb{L}^2(\mathbb{T},h)} \overset{(2.2)}{=} \left(u; \frac{DA_{m,l}}{\lambda_{m,l}}\right)_{\mathbb{L}^2(\mathbb{T},h)}$$

holds. We use the fact that the differential operator D is potentially self-adjoint in $\mathring{\mathbb{T}}$ and that the boundary is a set of measure zero. Due to the operator D to be potentially self-adjoint, we find a positive C^2-function g so that gD is self-adjoint, $\frac{1}{g}$ is well defined and symmetric. So we get

$$\left(u; \frac{DA_{m,l}}{\lambda_{m,l}}\right)_{\mathbb{L}^2(\mathbb{T},h)} = \left(u; \frac{(gD)A_{m,l}}{g \cdot \lambda_{m,l}}\right)_{\mathbb{L}^2(\mathbb{T},h)} = \frac{1}{\lambda_{m,l}} \left(\frac{1}{g}(gD)u; A_{m,l}\right)_{\mathbb{L}^2(\mathbb{T},h)}$$
$$\overset{\text{recursive}}{=} \left(\frac{1}{\lambda_{m,l}}\right)^k \left(D^k u; A_{m,l}\right)_{\mathbb{L}^2(\mathbb{T},h)}$$

and hence have shown

$$(A_{m,l}; A_{m,l})_{\mathbb{L}^2(\mathbb{T},h)} \cdot |\tilde{u}_{m,l}| = \left(\frac{1}{\lambda_{m,l}}\right)^k \left(D^k u; A_{m,l}\right)_{\mathbb{L}^2(\mathbb{T},h)}. \tag{4.4}$$

By this and

$$u(x,y) = \sum_{m,l \in \mathbb{N}_0} \tilde{u}_{m,l} A_{m,l}(x,y)$$

is satisfied for every point $(x,y) \in \mathbb{T}$, see [31, equation (18)], we get

$$\begin{aligned} |u(x,y) - u_N^\sigma(x,y)| &= \left| \sum_{\substack{0 \leq l+m \leq N \\ l,m \in \mathbb{N}_0}} \left(1 - \sigma\left(\frac{l+m}{N}\right)\right) \tilde{u}_{m,l} A_{m,l}(x,y) + \sum_{\substack{l+m > N \\ l,m \in \mathbb{N}_0}} \tilde{u}_{m,l} A_{m,l}(x,y) \right| \\ &= \left| \int_{\mathbb{T}} h(x_1,y_1) \left[S_N(x,y,x_1,y_1) + R_N(x,y,x_1,y_1) \right] D^k u(x_1,y_1) \, \mathrm{d}x_1 \, \mathrm{d}y_1 \right|, \end{aligned}$$

for the function u, where $S_N(x,y,x_1,y_1)$ and $R_N(x,y,x_1,y_1)$ are defined by

$$\begin{aligned} S_N(x,y,x_1,y_1) &= \sum_{\substack{1 \leq l+m \leq N \\ l,m \in \mathbb{N}_0}} \left(1 - \sigma\left(\frac{l+m}{N}\right)\right) \frac{A_{m,l}(x_1,y_1) A_{m,l}(x,y)}{||A_{m,l}||^2_{\mathbb{L}^2(\mathbb{T},h)} \lambda_{m,l}^k}, \\ R_N(x,y,x_1,y_1) &= \sum_{\substack{l+m > N \\ l,m \in \mathbb{N}_0}} \frac{A_{m,l}(x_1,y_1) A_{m,l}(x,y)}{||A_{m,l}||^2_{\mathbb{L}^2(\mathbb{T},h)} \lambda_{m,l}}. \end{aligned}$$

We apply the Cauchy-Schwarz inequality to estimate the integral. Therefore we have to estimate the weighted $\mathbb{L}^2(\mathbb{T})$-norms of S_N and R_N for all (x,y). For the R_N we extract the results from the proof of Theorem 3.1 from [31]. We summarize the results in Table 2. Now we are able to estimate the S_N. We follow the proof of

area	$\max\{\binom{l+p}{l}, \binom{l+\beta-1}{l}\}$	$\|\|R_N(x,y,\cdot,\cdot)\|\|_{\mathbb{L}^2(\mathbb{T},h)} <$
$\mathring{\mathbb{T}}$		$C_{R_1} N^{-2k+\frac{7}{4}}$
$[0,y]$	$\binom{l+p}{l}$	$C_{R_{2(1)}} N^{-2k+\frac{3}{2}\alpha+p+\frac{1}{2}}$
$[0,y]$	$\binom{l+\beta-1}{l}$	$C_{R_{2(2)}} N^{-2k+\frac{3}{2}\alpha+\beta-\frac{1}{2}}$
$[x,0]$		$C_{R_3} N^{-2k+\frac{3}{4}+\beta}$
$[x,1-x]$		$C_{R_4} N^{-2k+\frac{7}{4}+p}$
$(1,0)$		$C_{R_5} N^{-2k-\alpha+\gamma+\frac{3}{2}}$

TABLE 2. $C_{R_1}, \ldots, C_{R_5} \in \mathbb{R}^+$ are constants.

[31, Theorem 3.1] and start with some inner point $(x,y) \in \mathring{\mathbb{T}}$. It is

$$\begin{aligned}
||S_N(x,y,\cdot,\cdot)||^2_{\mathbb{L}^2(\mathbb{T},h)} &= \sum_{\substack{1\le l+m\le N\\ l,m\in\mathbb{N}_0}} \left(1-\sigma\left(\frac{l+m}{N}\right)\right)^2 \frac{A^2_{m,l}(x,y)}{||A_{m,l}||^2_{\mathbb{L}^2(\mathbb{T},h)}\lambda^{2k}_{m,l}} \\
&\overset{\substack{(2.3)\&\\(2.4)}}{\le} \sum_{\substack{1\le l+m\le N\\ l,m\in\mathbb{N}_0}} \left(1-\sigma\left(\frac{l+m}{N}\right)\right)^2 \frac{\kappa^2_{m,l}4(m+l+\gamma)^2\tilde{E}^2(x,y)}{\kappa^2_{l,m}(2l+\beta+p)^{\frac{1}{2}}(m+l)^{2k}(m+l+\gamma)^{2k}} \\
&\le 4\tilde{E}^2(x,y) \sum_{\substack{1\le l+m\le N\\ l,m\in\mathbb{N}_0}} \left(1-\sigma\left(\frac{l+m}{N}\right)\right)^2 \frac{1}{(m+l)^{2k+\frac{1}{2}}(m+l+\gamma)^{2k-2}}
\end{aligned}$$

Using the identity

$$\sum_{\substack{0<l+m\le N\\ l,m\in\mathbb{N}_0}} \left(\frac{1}{m+l}\right)^k = \sum_{i=1}^{N} \frac{i+1}{i^k}$$

as well as elementary estimates lead to

$$\begin{aligned}
||S_N(x,y,\cdot,\cdot)||^2_{\mathbb{L}^2(\mathbb{T},h)} &< 8\tilde{E}(x,y)^2 \sum_{i=1}^{N} \left(1-\sigma\left(\frac{i}{N}\right)\right)^2 \frac{1}{i^{4k-\frac{5}{2}}} \frac{N^{4k-\frac{5}{2}}}{N^{4k-\frac{5}{2}}} \\
&= 8\tilde{E}(x,y)^2 N^{-4k+\frac{7}{2}} \left(\frac{1}{N}\sum_{i=1}^{N} \left(1-\sigma\left(\frac{i}{N}\right)\right)^2 \left(\frac{i}{N}\right)^{-4k+\frac{5}{2}}\right).
\end{aligned}$$

If $N\to\infty$, the last factor conforms with the integral

$$\int_0^1 (1-\sigma(\tau))^2 \tau^{\frac{5}{2}-4k} \mathrm{d}\tau.$$

The integral is bounded by the given conditions. To verify this fact, we calculate the Taylor series of σ in 0. It is

$$\sigma(\tau) = \sum_{j=0}^{2k-1} \frac{1}{j!}\sigma^{(j)}(0)\tau^j + \mathrm{o}(\tau^{2k-1}) \quad \forall \tau\in[0,\varepsilon).$$

In connection with $\sigma(0)=1$ and $\sigma^{(j)}(0)=0$ for all $j=1,2,\dots,2k-2$ the term reduces to

$$\sigma(\tau) = 1 + \frac{1}{(2k-1)!}\sigma^{(2k-1)}(0)\tau^{2k-1} + \mathrm{o}(\tau^{2k-1})$$

for all $\tau\in[0,\varepsilon)$. Using this in the integral, we get

$$\int_0^{\varepsilon} \left(\frac{\sigma^{(2k-1)}(0)}{(2k-1)!}\tau^{2k-1} + \mathrm{o}(\tau^{2k-1})\right)^2 \tau^{-4k+\frac{5}{2}} \mathrm{d}\tau + \int_{\varepsilon}^1 (1-\sigma(\tau))^2\tau^{\frac{5}{2}-4k}\mathrm{d}\tau < C^2_{I_1},$$

because every part is bounded. Hence it applies

$$||S_N(x,y,\cdot,\cdot)||_{\mathbb{L}^2(\mathbb{T},h)} < \sqrt{8}\tilde{E}(x,y)N^{-2k+\frac{7}{4}}C_{I_1} = C_{S_1}N^{-2k+\frac{7}{4}},$$

and with the Cauchy-Schwarz inequality we show in total

$$\begin{aligned}|u(x,y)-u_N^\sigma(x,y)| \leq & ||D^k u||_{\mathbb{L}^2(\mathbb{T},h)} \left(||R_N(x,y,\cdot,\cdot)||_{\mathbb{L}^2(\mathbb{T},h)} + ||S_N(x,y,\cdot,\cdot)||_{\mathbb{L}^2(\mathbb{T},h)}\right) \\ \leq & \underbrace{(||D^k u||_{\mathbb{L}^2(\mathbb{T},h)})(C_{R_1}+C_{S_1})}_{K_1} N^{-2k+\frac{7}{4}}.\end{aligned}$$

The computations for the edges are analogously obtained. We present the results in the following table.

edge	$\max\{\binom{l+p}{l}, \binom{l+\beta-1}{l}\}$	$\lvert u(x,y)-u_N^\sigma(x,y)\rvert <$
$[0,y]$	$\binom{l+p}{l}$	$\frac{K_2}{N^{2k-\frac{3}{2}\alpha-p-\frac{1}{2}}}$,
$[0,y]$	$\binom{l+\beta-1}{l}$	$\frac{K_3}{N^{2k-\frac{3}{2}\alpha-\beta+\frac{1}{2}}}$,
$[x,0]$		$\frac{K_4}{N^{2k-\frac{3}{4}-\beta}}$
$[x,1-x]$		$\frac{K_5}{N^{2k-\frac{7}{4}-p}}$

For the last point $(1,0)$ we calculate it directly.

$$\begin{aligned}||S_N(1,0,\cdot,\cdot)||^2_{\mathbb{L}^2(\mathbb{T},h)} &= \sum_{m=1}^N \left(1-\sigma\left(\frac{m}{N}\right)\right)^2 \frac{A^2_{m,0}(1,0)}{||A_{m,0}||^2_{\mathbb{L}^2(\mathbb{T},h)}\lambda^{2k}_{m,0}} \\ &\overset{(2.3)}{<} 4\left(\frac{(\beta)_p\gamma^{\alpha-1}}{(1)_p}\right)\sum_{m=1}^N \left(1-\sigma\left(\frac{m}{N}\right)\right)^2 \frac{\binom{m+\gamma-\alpha}{m}^2}{m^{2k}(m+\gamma)^{2k-2}} \\ &< C_5 \sum_{m=1}^N \left(1-\sigma\left(\frac{m}{N}\right)\right)^2 \frac{1}{m^{2k}(m+\gamma)^{2k-2-2\gamma+2\alpha}} \frac{N^{4k-2-2\gamma+2\alpha}}{N^{4k-2-2\gamma+2\alpha}} \\ &< C_{S_5} N^{-4k+3+2\gamma-2\alpha}\left(\frac{1}{N}\sum_{m=1}^N \left(1-\sigma\left(\frac{m}{N}\right)\right)^2 \left(\frac{m}{N}\right)^{-4k+2+2\gamma-2\alpha}\right),\end{aligned}$$

and after all it ensues

$$|u(1,0)-u_N^\sigma(1,0)| < K_6 N^{-2k-\alpha+\gamma+\frac{3}{2}}.$$

□

4.2. **The Spectral Viscosity Method.** Since spectral methods are known to lack sufficient dissipation, Tadmor [38] proposed the Spectral Viscosity or Super-Spectral Viscosity Method (SV Method). The main idea of the SV Method is to add a small viscosity term to the conservation law (3.1). We show analogously to [25, 33] that by choosing a viscosity term which depends on the differential operator of the orthogonal basis, the SV Method can be seen as a spectral method with modal filtering.
For the SD scheme based on the APK expansions, we propose to consider high order operators of the form $(-D)^p$on the reference element $\mathbb{T}$. Let I_N be an index set and $\phi_k = A_{m,l}$ the APK polynomials in lexicographic order k, see section 3.

Theorem 4.4. *Let $N \in \mathbb{N}$ and $\{\phi_k | k \in I_N\}$ the APK polynomials on the triangle $\mathbb{T}$. The polynomials solve the eigenvalue problem*

$$-D\phi_k = -\lambda_k \phi_k, \tag{4.5}$$

where D is the differential operator of the polynomials. P_ϕ denotes the projection on the space of $\{\phi_k\}$. To solve the viscosity equation

$$\frac{\partial}{\partial t}u_N(\boldsymbol{x},t) + \nabla_{\boldsymbol{x}} \cdot P_\phi f(u_N(\boldsymbol{x},t)) = \varepsilon_N(-1)^{p+1}(-D)^p u_N(\boldsymbol{x},t) \tag{4.6}$$

by a splitting method is equivalent to multiply the coefficients $\hat{u}_k$ with the function

$$\sigma(k) = e^{-\varepsilon_N \Delta t \lambda_k^p}$$

in every update step of the equation

$$\frac{\partial}{\partial t}u_N(\boldsymbol{x},t) + \nabla_{\boldsymbol{x}} \cdot P_\phi f(u_N(\boldsymbol{x},t)) = 0.$$

Proof. We solve the equation (4.6) by a splitting method in two steps

$$\frac{\partial}{\partial t}u_N(\boldsymbol{x},t) = \varepsilon_N(-1)^{p+1}(-D)^p u_N(\boldsymbol{x},t) \tag{4.7}$$

and

$$\frac{\partial}{\partial t}u_N(\boldsymbol{x},t) + \nabla_{\boldsymbol{x}} \cdot P_\phi f(u_N(\boldsymbol{x},t) = 0 \tag{4.8}$$

With $u_N(\boldsymbol{x},t) = \sum\limits_{k\in I_N} \hat{u}_k\phi_k(\boldsymbol{x})$ equation (4.7) implies

$$\sum_{k\in I_N} \frac{\partial \hat{u}_k}{\partial t}\phi_k(\boldsymbol{x}) = \sum_{k\in I_N} \varepsilon_N(-1)^{p+1}\hat{u_k}(-D)^p\phi_k(\boldsymbol{x}) = \sum_{k\in I_N} -\varepsilon_N\hat{u}_k(t)\lambda_k^p\phi_k(\boldsymbol{x}),$$

where we applied the eigenvalue equation (4.5) in the last step. By comparing the coefficients we have to solve the ordinary differential equations

$$\frac{\partial \hat{u}_k(t)}{\partial t} = -\varepsilon_N\hat{u_k}(t)\lambda_k^p, \quad \forall k \in I_N.$$

The solution is $\hat{u}_k(t) = ce^{-\varepsilon_N\lambda_k^p t}$, $c \in \mathbb{R}$. With $\Delta t := t^{n+1} - t^n$ and the requirement $\hat{u}_k(t^{n+1}) = \hat{u}_k(t^n)$ for $\Delta t = 0$ follows

$$\hat{u}_k(t^{n+1}) = e^{-\varepsilon_N\lambda_k^p(\Delta t + t^n)} = \underbrace{e^{(-\varepsilon_N\lambda_k^p\Delta t)}}_{=:\sigma(k)}\hat{u}_k(t^n).$$

□

In order of us to speak of a modal filter for $\sigma(k) = \sigma((l,m)) = e^{-\varepsilon_N(l+m)^p(l+m+\gamma)^p\Delta t}$, we have to multiply the exponenet with N^{2p}, meaning

$$\sigma\left(\frac{l+m}{N}\right) = e^{-\varepsilon_N N^{2p}\left(\frac{l+m}{N}\right)^p\left(\frac{l+m+\gamma}{N}\right)^p\Delta t} \approx e^{-\varepsilon_N N^{2p}\Delta t\left(\frac{l+m}{N}\right)^{2p}}. \tag{4.9}$$

Hence $\sigma : [0,1] \to [0,1]$ can be seen as an exponential filter of order $2p$ with filter strength $\alpha_i := -\varepsilon_N N^{2p}\Delta t$. We consider (4.9) in detail and realize that our modal filter depends on the parameter γ of the APK polynomials, especially if the polynomials have minor degree. So for different families of APK polynomials we get various specific modal filters.
We can prove similar results to theorem 4.4 for every orthogonal basis $\{\phi_k\}$, if the ϕ_k fulfil a comparable eigenvalue equation.
For the transfer of the SV Method to our Spectral Difference Method we follow the steps according to [47]. The transformation T_i from τ_i to $\mathbb{T}$ has no effect on the

flux function, so that the SD update scheme of a scalar hyperbolic equation in the cell τ_i with viscosity term and the solution points $\xi_j \in \mathbb{T}$ reads like

$$\begin{aligned} &\frac{\partial}{\partial t} u_N(T_i^{-1}(\boldsymbol{\xi}_j, t)) + \nabla_{\boldsymbol{\xi}} \cdot \tilde{P}_N(J_{T_i})^T \tilde{F}(u_N(T_i^{-1}(\boldsymbol{\xi}_j), t)) \\ =&\varepsilon_N (-1)^{p+1} (-D)^p (u_N(T_i^{-1}(\boldsymbol{\xi}_j), t)), \end{aligned} \tag{4.10}$$

where $\tilde{F}$ is the flux function, $\tilde{P}$ is the projection and $\nabla_{\boldsymbol{\xi}}$ is the nabla operator on $\mathbb{T}$. The same approach as in theorem 4.4 yields the equivalent of (4.10) and the SD Method with the modal filter (4.9).
Hence, the matrix representation (3.7) for the SD update scheme in cell τ_i becomes

$$\begin{aligned} \frac{\mathrm{d}\mathbf{u}^s}{\mathrm{d}t}(t) =& -(\xi_x D_\xi + \xi_y D_\eta)\big(\sigma(k)\hat{F}_{k,1}(t)\big)_k \\ &-(\eta_x D_\xi + \eta_y D_\eta)\big(\sigma(k)\hat{F}_{k,2}(t)\big)_k \\ =& -(\xi_x D_\xi + \xi_y D_\eta) M_\sigma \hat{\mathbf{F}}_1(t) \\ &-(\eta_x D_\xi + \eta_y D_\eta) M_\sigma \hat{\mathbf{F}}_2(t) \\ =& -(\xi_x D_\xi + \xi_y D_\eta) M_\sigma \mathcal{V}^{-1} \mathbf{F}_1(t) \\ &-(\eta_x D_\xi + \eta_y D_\eta) M_\sigma \mathcal{V}^{-1} \mathbf{F}_2(t) \end{aligned} \tag{4.11}$$

with viscosity, where $M_\sigma := \mathrm{diag}(\sigma(1), \dots, \sigma(N_F))$ is a diagonal matrix. So we have to choose the size of ε_N, thereby we stick on the analysis of [9]. The authors suggested in the Fourier case a viscosity strength ε_N, which depends on the approximation order as

$$\varepsilon_N \sim \frac{C_P}{N^{2p-1}},$$

where the constant C_P may be chosen by

$$C_p \leq \sum_{k=1}^{p} ||\partial_u^k (J_{T_i})^T \tilde{F}(u)||_{\mathbb{L}^\infty} = ||(J_{T_i})^T||_\infty \sum_{k=1}^{p} ||\partial_u^k \tilde{F}(u)||_{\mathbb{L}^\infty}.$$

Here, we ignore the dependence on u and approximate $||(J_{T_i})^T||_\infty \sim \frac{1}{h_i}$ by a measure of length h_i of the triangle τ_i. Finally we arrive at

$$\varepsilon_N^i := \frac{c}{h_i N^{2p-1}} < \frac{\sum_{k=1}^{p} ||\partial_u^k \tilde{F}(u)||_{\mathbb{L}^\infty}}{h_i N^{2p-1}}, \tag{4.12}$$

where $c \in \mathbb{R}$ is a constant. We have to select the constant c and the filter order $2p$ in our numerical tests.

Remark 4.5. The numerical tests from [29, 47] imply that we have to increase c if we enlarge the filter order $2p$.
Furthermore, it is a known fact that the application of a modal filter in the global domain will destroy the order of convergence. Shock indicators are used to detect corrupted cells. There are different approaches to detect jumps in a cell, see [32, 48] for example. Here we use the shock indicator of [3]. The indicator compares the higher coefficients with the lower ones to detect oscillations.

In general, the time step Δt in the explicit time-stepping scheme[4] for the resulting ODEs (in t) at each solution point $\mathbf{x}_j$, which also appears in the filter strength $\alpha_i = -\varepsilon_N N^{2p}\Delta t$ in (4.9), can't be chosen arbitrarily. For a scalar conservation law $u_t(x,t) + \lambda u_x(x,t) = 0$ in one space dimension and a numerical scheme on a uniform grid with length h one should choose Δt small enough, so that a wave with propagation speed λ can't travel more than h in one time step. I.e. the *Courant-Friedrichs-Levy condition* $\lambda\Delta t \leq h$ has to hold. The maximum

$$\max_{\lambda} \frac{\lambda\Delta t}{h} =: \mathrm{CFL}$$

is called *Courant number* and the following example gives a first intuition how it can determined on a triangulation.

Example 4.6. We observe the two dimensional advection equation

$$u_t(x,y,t) + u_x(x,y,t) + u_y(x,y,t) = 0.$$

Here the propagation speed in $(1,1)$ direction is $\sqrt{2}$, which leads to the Courant number $\mathrm{CFL} = \frac{\sqrt{2}\Delta t}{h}$, in which h is now a measure of length of the observed triangle.

As we can see in section 5.2 the SD Method has stability problems for all parameters α, β and γ, which are increasing for rising order N. Hence, we can't even compute a sufficiently numerical Courant number and will choose the time step

$$\Delta t := \frac{C_{fix}}{(N+1)^2} \cdot \frac{h}{\lambda_{max}} \tag{4.13}$$

with a fixed value C_{fix} and maximal propagation speed λ_{max}. Therefore, the time step adapts an increasing instability for rising N, the "geometry" of the triangulation by h and by $C_{fix} = \frac{1}{2}$, which will be our choice, (4.13) coincides with the Courant number in example 4.6 for $N = 0$.

5. Stability of the Spectral Difference Method

By von Neumann analysis in matrix form for a scalar advection equation in two spatial dimensions with periodic initial condition, one can observe the linear stability of the semi-discretization. This was already done by Abeele, Lacor and Wang for the classical SD Method in [40], by Huynh for the FR Method in [15] and many other authors. Here we observe the SD Method for APK polynomials on a triangular grid, which is generated by a pattern like in figure 2 for a scalar advection equation

$$u_t + \cos(\psi)u_x + \sin(\psi)u_y = 0$$

with $\psi \in [0, \frac{\pi}{2}]$ and the periodic initial condition

$$u_{init}(x,y) = e^{I(w_x x + w_y y)},$$

where $w_x, w_y \in [-\pi, \pi]$ are the so called *wave numbers* in x- and y-direction. The exact solution is then given by

$$u_{exact}(x,y,t) = e^{I(w_x x + w_y y - [w_x \cos\psi + w_y \sin\psi]t)} \tag{5.1}$$

[4]We already mentioned, that we use the 4-th order low storage Runge-Kutta scheme defined by Carpenter and Kennedy (see [5]) in our implementation for section 6.

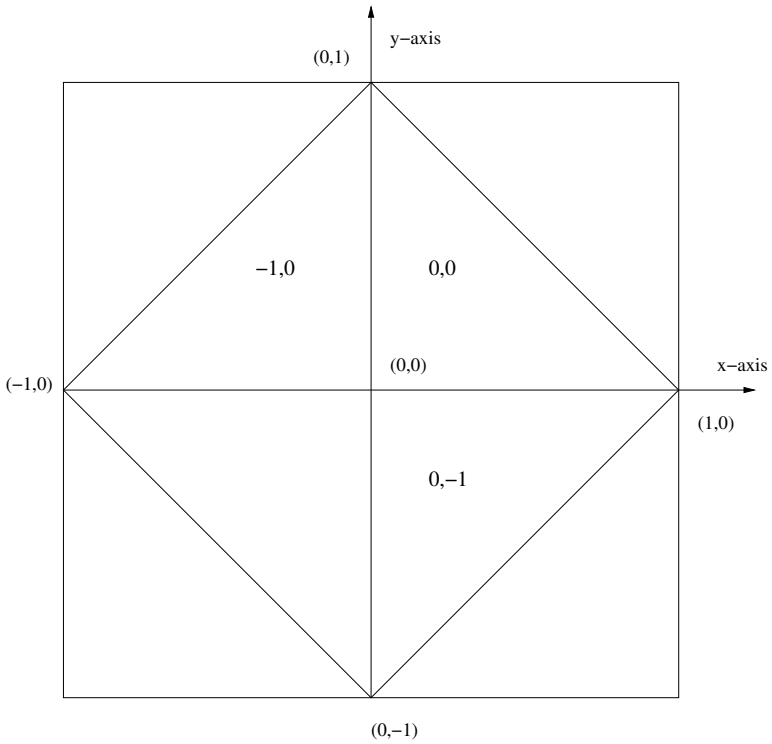

FIGURE 2. Generating pattern

for $t \geq 0$. We will concentrate on the semi discretization at $t = 0$ and wish to obtain a relation in form of a linear ODE system

$$\frac{\mathrm{d}\mathbf{u}^s}{\mathrm{d}t} = S\mathbf{u}^{\mathbf{s}} \tag{5.2}$$

of first order and with constant coefficients in the solution points. Similar to the scalar case $\frac{\mathrm{d}u}{\mathrm{d}t} = \lambda u$, where the solution is given by $u(t) = ce^{\lambda t}$ for $c \in \mathbb{R}$, the eigenvalues of the matrix S take the place of λ. Hence the asymptotic behavior of the solution of (5.2) depends on the real parts of the eigenvalues: If all eigenvalues of S lie in the left half of the complex plane, the solution is bounded, which coincides with the behavior of the exact solution u_{exact}. In this case we call the semi discretization to be *stable*. On the other hand, if any eigenvalue lies in the right half of the complex plane, the solution of (5.2) will blow up for $t \to \infty$ and so might the scheme. This will happen unless the *instability* is mild, i.e. $\max_{\lambda} \mathrm{Re}(\lambda)$ is small, and the time steps adapt to this and are sufficiently small. In 5.1 we will first derive a matrix representation like (5.2) for the SD scheme at $t = 0$ and for the test case above. In 5.2 we will analyze the stability of the unfiltered SD scheme from section 3 for certain ranges for α, β and γ. By observation of the numerical test cases, one can see that some stabilization is necessary and we did so in section 4 by the SV Method in terms of the SD Method with modal filtering. Following this, in 5.3 we will do a similar analysis to 5.2 for the SD Method with modal filtering. One can see how the modal filtering leads to much better stability properties and

how they depend on certain parameters like the order p and α, β, γ from the APK polynomials.

5.1. **Matrix representation.** We already stated in section 3 that the universal update scheme (3.3) at the cell $\tau_{i,j}$ reads

$$\frac{\mathrm{d}\mathbf{u}^s_{i,j}(t)}{\mathrm{d}t} = -(\xi_x D_\xi + \xi_y D_\eta)\mathcal{V}^{-1}\mathbf{F}_1(t) - (\eta_x D_\xi + \eta_y D_\eta)\mathcal{V}^{-1}\mathbf{F}_2(t), \tag{5.3}$$

when evaluated at the solution points. If we look at the cell $\tau_{0,0}$ and denote $\frac{\mathrm{d}\mathbf{u}^s_{i,j}(t=0)}{\mathrm{d}t}$ for sake of simplicity by $\frac{\mathrm{d}\mathbf{u}^s}{\mathrm{d}t}$ equation (5.3) becomes

$$\frac{\mathrm{d}\mathbf{u}^s}{\mathrm{d}t} = -(D_\xi \mathcal{V}^{-1}\mathbf{F}_1 + D_\eta \mathcal{V}^{-1}\mathbf{F}_2), \tag{5.4}$$

since $\tau_{0,0}$ and its neighbors are parametrized by the orientation-preserving affine transformations

$$T_{0,0}(x,y) = \begin{pmatrix} x \\ y \end{pmatrix}, T_{-1,0}(x,y) = \begin{pmatrix} y \\ -x \end{pmatrix}, T_{0,-1}(x,y) = \begin{pmatrix} -y \\ x \end{pmatrix}, T_{0,1}(x,y) = \begin{pmatrix} 1-x \\ 1-y \end{pmatrix}.$$

Note that $\mathbf{F}_1, \mathbf{F}_2$ are given by (3.6), where the upwind flux is used and the flow direction was restricted to $\psi \in [0, \frac{\pi}{2}]$. Consequently $\mathbf{F}_1, \mathbf{F}_2$ are independent of the values from $\tau_{0,1}$ and so (5.4) now reads

$$\begin{aligned}\frac{\mathrm{d}\mathbf{u}^s}{\mathrm{d}t} =& -\cos(\psi) D_\xi \mathcal{V}^{-1}\big[M_1^{-1,0}\mathbf{u}^f_{-1,0} + M_1^{0,0}\mathbf{u}^f_{0,0} + M_1^{0,-1}\mathbf{u}^f_{0,-1}\big] \\ & -\sin(\psi) D_\eta \mathcal{V}^{-1}\big[M_2^{-1,0}\mathbf{u}^f_{-1,0} + M_2^{0,0}\mathbf{u}^f_{0,0} + M_2^{0,-1}\mathbf{u}^f_{0,-1}\big].\end{aligned}$$

Here the $M_i^{m,n}$ for the second order SD Method, and so $K_F = \frac{(2+1)(2+2)}{2} = 6$, are

$$\begin{aligned} M_1^{-1,0} &= e_1^T e_1 + e_2^T e_2 + e_3^T e_3,\ M_1^{0,0} = e_5^T e_5 + e_6^T e_6,\ M_1^{0,-1} = e_4^T e_4, \\ M_2^{-1,0} &= e_2^T e_2,\ M_2^{0,0} = e_3^T e_3 + e_5^T e_5,\ M_2^{0,-1} = e_1^T e_1 + e_4^T e_4 + e_6^T e_6. \end{aligned}$$

For the exact computation see [47, chapter 3.3.1] and the $M_i^{m,n}$ for $N = 3, 4, 5$ can be found in the appendix. Next we can make use of the periodicity of the initial condition to get rid of $\mathbf{u}^f_{-1,0}$ and $\mathbf{u}^f_{0,-1}$ by substituting them by terms $T_{-1,0}\mathbf{u}^f_{0,0}$ and $T_{0,-1}\mathbf{u}^f_{0,0}$. Therefore, note that $\mathbf{u}^f_{-1,0}, \mathbf{u}^f_{0,0}$ and $\mathbf{u}^f_{0,-1}$ are given by the initial condition. Hence

$$\begin{aligned} \mathbf{u}^f_{0,0} =& (u_{init}(T_{0,0}^{-1}(\xi_k, \eta_k)))_k = (u_{init}(\xi_k, \eta_k))_k \\ =& (e^{I(w_x\xi_k + w_y\eta_k)})_k, \\ \mathbf{u}^f_{-1,0} =& (u_{init}(T_{-1,0}^{-1}(\xi_k, \eta_k)))_k = (u_{init}(-\eta_k, \xi_k))_k \\ =& (e^{I(-w_x\eta_k + w_y\xi_k)})_k = (e^{I(-w_x(\xi_k+\eta_k)+w_y(\xi_k-\eta_k))} \cdot e^{I(w_x\xi_k + w_y\eta_k)})_k \\ =& T_{-1,0}\mathbf{u}^f_{0,0}, \\ \mathbf{u}^f_{0,-1} =& (u_{init}(T_{0,-1}^{-1}(\xi_k, \eta_k)))_k = (u_{init}(\eta_k, -\xi_k))_k \\ =& (e^{I(w_x\eta_k - w_y\xi_k)})_k = (e^{I(w_x(\eta_k-\xi_k)-w_y(\xi_k+\eta_k))} \cdot e^{I(w_x\xi_k + w_y\eta_k)})_k \\ =& T_{0,-1}\mathbf{u}^f_{0,0} \end{aligned}$$

with

$$T_{-1,0} := \sum_k e^{I(-w_x(\xi_k+\eta_k)+w_y(\xi_k-\eta_k))} e_k^T e_k,$$
$$T_{0,-1} := \sum_k e^{I(w_x(\eta_k-\xi_k)-w_y(\xi_k+\eta_k))} e_k^T e_k,$$

and we obtain

$$\begin{aligned}\frac{\mathrm{d}\mathbf{u}^s}{\mathrm{d}t} = -\Big(&\cos(\psi) D_\xi \mathcal{V}^{-1}\big[M_1^{-1,0}T_{-1,0} + M_1^{0,0} + M_1^{0,-1}T_{0,-1}\big] \\ &+ \sin(\psi) D_\eta \mathcal{V}^{-1}\big[M_2^{-1,0}T_{-1,0} + M_2^{0,0} + M_2^{0,-1}T_{0,-1}\big]\Big)\mathbf{u}_{0,0}^f.\end{aligned} \tag{5.5}$$

Last, we want to write $\mathbf{u}_{0,0}^f$ in terms of $\mathbf{u}_{0,0}^s$ or just $\mathbf{u}^s$ to obtain a relation as in (5.2). While we reconstructed the flux F by APK polynomials, in order to later use their natural filter given by (4.9), we reconstruct the solution u by Lagrange polynomials. Hence

$$\begin{aligned}\mathbf{u}_{0,0}^f =& \Big(\sum_{k=1}^{K_s} u_{0,0}(\mathbf{x}_k^s) L_k(T_{0,0}(\mathbf{x}_j^f))\Big)_j^{K_F} \\ =& E_{Lag}\mathbf{u}^s\end{aligned}$$

with

$$E_{Lag} := \big(L_k(\mathbf{x}_j^f)\big)_{j,k} \in \mathbb{R}^{K_F \times K_s}.$$

If we use that in (5.5) we finally obtain

$$\begin{aligned}\frac{\mathrm{d}\mathbf{u}^s}{\mathrm{d}t} = -\Big(&\cos(\psi) D_\xi \mathcal{V}^{-1}\big[M_1^{-1,0}T_{-1,0} + M_1^{0,0} + M_1^{0,-1}T_{0,-1}\big] \\ &+ \sin(\psi) D_\eta \mathcal{V}^{-1}\big[M_2^{-1,0}T_{-1,0} + M_2^{0,0} + M_2^{0,-1}T_{0,-1}\big]\Big)E_{Lag}\mathbf{u}^s,\end{aligned}$$

which we want to retain in the following lemma.

Lemma 5.1. *For a linear advection equation with flow direction $\psi \in [0, \frac{\pi}{2}]$ and periodic initial condition u_{init} on a triangular grid like in figure 2, where the fully upwind is used, the universal update scheme (3.3) on $\tau_{0,0}$ reads*

$$\frac{\mathrm{d}\mathbf{u}^s}{\mathrm{d}t} = S\mathbf{u}^s$$

with semi-discretization S given by

$$\begin{aligned}S := -\Big(&\cos(\psi) D_\xi \mathcal{V}^{-1}\big[M_1^{-1,0}T_{-1,0} + M_1^{0,0} + M_1^{0,-1}T_{0,-1}\big] \\ &+ \sin(\psi) D_\eta \mathcal{V}^{-1}\big[M_2^{-1,0}T_{-1,0} + M_2^{0,0} + M_2^{0,-1}T_{0,-1}\big]\Big)E_{Lag}.\end{aligned} \tag{5.6}$$

We already stated in section 4 that the universal update scheme (3.3) with modal filtering at the cell $\tau_{i,j}$ reads

$$\begin{aligned}\frac{\mathrm{d}\mathbf{u}_{i,j}^s(t)}{\mathrm{d}t} =& -(\xi_x D_\xi + \xi_y D_\eta) M_\sigma \mathcal{V}^{-1}\mathbf{F}_1(t) \\ &- (\eta_x D_\xi + \eta_y D_\eta) M_\sigma \mathcal{V}^{-1}\mathbf{F}_2(t),\end{aligned} \tag{5.7}$$

when evaluated at the solution points. If we combine this with lemma 5.1, we obtain a similar corollary for the the filtered SD Method.

Corolla 5.2. *For a linear advection equation with flow direction $\psi \in [0, \frac{\pi}{2}]$ and periodic initial condition u_{init} on a triangular grid like in figure 2, where the full upwind is used, the universal update scheme with modal filtering on $\tau_{0,0}$ reads*

$$\frac{\mathrm{d}\mathbf{u}^s}{\mathrm{d}t} = S_\sigma \mathbf{u}^s$$

with semi discretization S_σ given by

$$\begin{aligned} S_\sigma := -\Big(&\cos(\psi) D_\xi M_\sigma \mathcal{V}^{-1}\big[M_1^{-1,0}T_{-1,0} + M_1^{0,0} + M_1^{0,-1}T_{0,-1}\big] \\ &+ \sin(\psi) D_\eta M_\sigma \mathcal{V}^{-1}\big[M_2^{-1,0}T_{-1,0} + M_2^{0,0} + M_2^{0,-1}T_{0,-1}\big]\Big) E_{Lag}. \end{aligned} \tag{5.8}$$

5.2. **Stability Analysis for the SD Method.** We already stated that the asymptotic behavior of the solution of (5.2) depends on the real parts of the eigenvalues of $S \equiv S(\alpha, \beta, \gamma)$ given by (5.6). For linear stability, we wish them to lie in the left half of the complex plane. In case there are no such parameters $\alpha, \beta \in \mathbb{R}^+$ and $\gamma > \alpha + \beta - 1$, we want at least to find a set of parameters (α, β, γ) with preferably small real parts. If we denote the maximal real part over all eigenvalues corresponding to a certain parameter set (α, β, γ) and a fixed set of test cases with respect to w_x, w_y, ψ by $\Lambda \equiv \Lambda(\alpha, \beta, \gamma)$, this leads to the optimization problem

$$\underset{\alpha,\beta\in\mathbb{R}^+,\gamma>\alpha+\beta-1}{\arg\min} \quad \Lambda(\alpha, \beta, \gamma). \tag{5.9}$$

Note that this is a continuous and non-convex problem. Future studies could give a strict treatment of the optimization problem (5.9), but since we just want to demonstrate the influence of the chosen polynomial basis on the stability of the SD Method with and without modal filtering, we will just concentrate on certain subranges for α, β and γ. In the following, we will concentrate on the subrange of

$$P := \{(\alpha, \beta, \gamma) \mid \alpha, \beta = 0.1, 0.2, \ldots, 2 \text{ and } \gamma = \alpha + \beta, \alpha + \beta + 0.1, \ldots, 6\}$$

due to the observation that higher parameters lead to much worse condition numbers, see 1. For a fixed parameter set (α, β, γ) in such a subrange we will compute all eigenvalues of S and look for the one with the greatest real part. This will be done for several test cases with respect to the flow direction $\psi \in [0, \frac{\pi}{2}]$ and the wave numbers $w_x, w_y \in [-\pi, \pi]$. Then we will again look after the greatest real part among all these test cases. The resulting eigenvalue and its real part will be taken as an evidence for the stability of the underlying parameter set (α, β, γ) and its corresponding polynomial basis. All of this is done in MatLab, where a descriptive pseudo code is given by Algorithm 1. The numerical results show that the maximal real part of all eigenvalues L is independent of α, β and γ. Hence the linear stability is independent of the corresponding basis of APK polynomials, which coincides with the following theorem.

Theorem 5.3. *In Lemma 5.1 the eigenvalues of the semi-discretization S, given by (5.6), are independent of the basis of APK polynomials corresponding to α, β and γ.*

Proof. Looking at S, only the differential matrices D_ξ, D_η, given by (3.5), and the Vandermonde matrix $\mathcal{V}$, coming from the interpolation approach, depend on the underlying basis $\{\phi_k \mid 1 \le k \le K_F\}$ of $\mathbb{P}_N(\mathbb{T})^2$. Hence the proof is done, when we

Algorithm 1 without filtering

for $\alpha, \beta = 0.1 : 0.1 : 2,\ \gamma = \alpha + \beta : 0.1 : 6$ **do**
  $L << 0$ (e.g. -42)
  for $\psi = 0 : \frac{\pi}{8} : \frac{\pi}{2},\ w_x, w_y = -\pi : \frac{\pi}{2} : \pi$ **do** ▷ test cases
    compute S
    v = eig(S)
    v_{re} = real(v)
    $\Lambda = \max(\mathrm{v}_{re})$
    if $\Lambda > L$ **then**
      $L = \Lambda$
  return $(\alpha, \beta, \gamma, L)$ ▷ L is the greatest real part

can eliminate this matrices from S. Therefore note that

$$\begin{aligned} D_\xi &= \Big(\partial_\xi \phi_k\big(T_{0,0}(\mathbf{x}_j^s)\big)\Big)_{j,k}^{K_s,K_F} \\ &= \big(\partial_\xi \phi_k(\boldsymbol{x})|_{\boldsymbol{x}=\mathbf{x}_j^s}\big)_{j,k} \\ &= \Big(\partial_\xi \big[\sum_{i=1}^{K_F} \phi_k(\mathbf{x}_i^F) L_i(\boldsymbol{x})\big]|_{\boldsymbol{x}=\mathbf{x}_j^s}\Big)_{j,k} \\ &= \big(\sum_{i=1}^{K_F} \phi_k(\mathbf{x}_i^F)\partial_\xi L_i(\boldsymbol{x})|_{\boldsymbol{x}=\mathbf{x}_j^s}\big)_{j,k} \\ &= \big(\partial_\xi L_i(\mathbf{x}_j^s)\big)_{j,i}^{K_s,K_F} \cdot \big(\phi_k(\mathbf{x}_i^F)\big)_{i,k}^{K_F,K_F} \\ &= D_\xi^{Lag}\mathcal{V} \end{aligned}$$

and analogous $D_\eta = D_\eta^{Lag}\mathcal{V}$ with

$$D_\xi^{Lag} := \big(\partial_\xi L_i(\mathbf{x}_j^s)\big)_{j,i}^{K_s,K_F}\ ,\ D_\eta^{Lag} := \big(\partial_\eta L_i(\mathbf{x}_j^s)\big)_{j,i}^{K_s,K_F}$$

independent of the basis $\{\phi_k\}$. Hence

$$D_\xi \mathcal{V}^{-1} = D_\xi^{Lag}\ ,\ D_\eta \mathcal{V}^{-1} = D_\eta^{Lag} \tag{5.10}$$

and

$$\begin{aligned} S = -\big(&\cos(\psi) D_\xi^{Lag}[M_1^{-1,0}T_{-1,0} + M_1^{0,0} + M_1^{0,-1}T_{0,-1}] \\ &+ \sin(\psi) D_\eta^{Lag}[M_2^{-1,0}T_{-1,0} + M_2^{0,0} + M_2^{0,-1}T_{0,-1}]\big)E_{Lag} \end{aligned} \tag{5.11}$$

is independent of the underlying basis $\{\phi_k\}$. □

Note that we have done the proof for an arbitrary basis $\{\phi_k\}$ of $\mathbb{P}_N(\mathbb{T})^2$ and that by (5.10) moreover the more general universal update scheme (3.7) for a general (non-linear) conservation law becomes

$$\frac{\mathrm{d}\mathbf{u}^s}{\mathrm{d}t}(t) = -(\xi_x D_\xi^{Lag} + \xi_y D_\eta^{Lag})\mathbf{F}_1(t) - (\eta_x D_\xi^{Lag} + \eta_y D_\eta^{Lag})\mathbf{F}_2(t)$$

with $\mathbf{F}_1(t), \mathbf{F}_2(t)$ independent of the basis $\{\phi_k\}$, when we use an interpolation approach to reconstruct the flux. This leads to the following corollary.

Corolla 5.4. *The SD Method (without filtering) with a interpolation approach is independent of the underlying polynomial basis.*

Remark 5.5. While the SD Method with an interpolation approach theoretically is independent of the underlying polynomial basis, in computation their condition properties may have an influence on the resulting scheme, see table 1. By substituting D_ξ by D_ξ^{Lag} and D_η by D_η^{Lag} and working with (5.11) in our implementation, we blind out condition properties of the underlying basis and just focus on the pure stability properties of the SD Method. However, one should note that this won't be the case in the next subsection, where the Vandermonde matrix and its inverse will not cancel out each other. Then, to cover condition issues as well, we focus on a proper subrange of parameters which will ensure good condition numbers. In such a subrange we then will optimize the linear stability of the SD Method.

Table 3 shows the maximal real parts among all test cases for certain orders N. These values show that the SD Method on triangles is not stable, independent of

N	maximal real part L
2	5.228025e+00
3	7.671293e+00
4	1.360921e+01
5	2.010942e+01

TABLE 3. maximal real parts

the polynomial basis in the interpolation approach. This was already stated by Van den Abeele, Lacor and Wang in [40]. As one can see in Table 3 the instabilities, i.e. $\mathrm{Re}(\lambda)$, of the method can be 'quite high'. To deal with this problem we will apply the modal filter in the SD Method in the next section.

5.3. **Numerical Stability Analysis for the SD Method with Modal Filtering.** As we proposed in section 4, we use the SV Method seen as a spectral method with modal filtering to obtain milder instabilities in the von Neumann analysis and hence preserving the scheme to blow up at discontinuities. While we used $D\mathcal{V}^{-1} = D^{Lag}$ in section 5.2 to show that the SD Method is independent of the underlying basis this term becomes

$$DM_\sigma \mathcal{V}^{-1}$$

in the semi discretization S_σ, given by (5.8), for the SD Method with modal filtering. This again leads to $S_\sigma \equiv S_\sigma(\alpha, \beta, \gamma)$ and the method to depend on the corresponding basis of APK polynomials. Following section 5.2 we use Algorithm 1 with $S = S_\sigma$ for a (linear) stability analysis for the SD Method with modal filtering. But first, note that the values of the modal filter σ in the filter matrix $M_\sigma := \mathrm{diag}(\sigma_1, \ldots, \sigma_{K_F})$ depend on certain constants, which were explained in section 4.2. For the following numerical results we set

$$h = \frac{\sqrt{2}}{6}, \quad \text{see (4.12)},$$
$$C_{fix} = \frac{1}{2}, \quad \lambda_{\max} = 1, \quad \text{see (4.13)}.$$

For order $N = 3$, different orders $p \in \mathbb{N}_1^5$ and constants $c \in \mathbb{N}_2^8$ in the filter strength (4.12), table 4 - 6 shows the smallest real parts L (maximum over all test cases) and their corresponding parameters $(\alpha, \beta, \gamma) \in P$. We can see in Tables 4 - 6 that

p	c	(α,β,γ)	L
1	2	(2,2,6)	4.474928e+00
	3	(2,2,6)	3.452260e+00
	4	(2,2,6)	2.825792e+00
	5	(2,2,6)	2.341697e+00
	6	(2,2,4.2)	1.949950e+00
	7	(2,2,4.5)	1.630852e+00
	8	(2,2,4.6)	1.378782e+00
p	c	(α,β,γ)	L
2	2	(2,2,5.2)	2.500718e+00
	3	(2,2,5)	2.000045e+00
	4	(2,2,4.7)	1.783495e+00
	5	(2,2,5.7)	1.576658e+00
	6	(2,2,5.5)	1.398979e+00
	7	(2,2,5.3)	1.242022e+00
	8	(2,2,5.1)	1.111981e+00

TABLE 4. maximal real parts for $p = 1$ and $p = 2$

p	c	(α,β,γ)	L
3	2	(2,2,4.6)	2.137056e+00
	3	(2,2,5.5)	1.826333e+00
	4	(2,2,5.2)	1.560388e+00
	5	(1.1,1.1,6)	1.349429e+00
	6	(1.1,1.1,6)	1.181007e+00
	7	(1,1.1,6)	1.050789e+00
	8	(1,1,6)	9.382501e-01
p	c	(α,β,γ)	L
4	2	(2,2,5.4)	1.836013e+00
	3	(2,2,5.1)	1.511921e+00
	4	(2,2,4.7)	1.339156e+00
	5	(1,1,5.9)	1.187603e+00
	6	(1,1,5.9)	1.094414e+00
	7	(1,1,5.9)	1.029666e+00
	8	(1,1,5.9)	9.742486e-01

TABLE 5. maximal real parts for $p = 3$ and $p = 4$

one can obtain much milder instabilities of the method by modal filtering, where also the choice of family of APK polynomials for the underlying basis of $\mathbb{P}_N(\mathbb{T})^2$ has an influence. Note that in fact both p, c and every parameter α, β and γ effect the linear stability. Approximately, the parameter tuples $(1, 1, 6)$ and $(2, 2, 5)$ appear promising. However, by considering their conditional numbers in table 1, the parameter tuple $(1, 1, 6)$ becomes unreasonable, due to its high condition numbers. Thus, we will focus on parameter tuple $(2, 2, 5)$ in the following example which will help us to find suitable choices for the parameter c and the filter order p.

p	c	(α, β, γ)	maximal real part L
5	2	(2,2,5)	1.525311e+00
	3	(1,1,5.9)	1.355060e+00
	4	(2,2,4.3)	1.186385e+00
	5	(2,2,4.1)	1.075861e+00
	6	(2,2,4)	1.100214e+00
	7	(1,1,5.9)	1.097985e+00
	8	(1,1,5.9)	1.056802e+00

TABLE 6. maximal real parts for $p = 5$

Example 5.6. First, we observe that the constant c has an influence on the linear stability by comparing the parameter tuple $(2, 2, 5)$ for $N = 3$, $p = 2$ and different c. In this case we have

$$\begin{aligned} L &= 2.502205e + 00 \text{ for } c = 2, \\ L &= 2.000045e + 00 \text{ for } c = 3, \\ L &= 1.824525e + 00 \text{ for } c = 4, \\ L &= 1.639219e + 00 \text{ for } c = 5, \\ L &= 1.459258e + 00 \text{ for } c = 6, \\ L &= 1.290925e + 00 \text{ for } c = 7, \\ L &= 1.135887e + 00 \text{ for } c = 8, \end{aligned}$$

which indicates that by increasing parameter c the instability gets milder. This coincides with theorem 4.4 which states the equivalence of modal filtering by our natural filters and the SV Method. In this formulation c is proportional to ε_N, see (4.12), which again is proportional to the dissipation we add to the underlying conservation law by the viscosity term.

In the same way, by comparing the parameter tuple $(2, 2, 5)$ for $N = 3$ and $c = 8$, we can observe the influence of the parameter p. Here

$$\begin{aligned} L &= 1.406930e + 00 \text{ for } p = 1, \\ L &= 1.135887e + 00 \text{ for } p = 2, \\ L &= 1.227645e + 00 \text{ for } p = 3, \\ L &= 1.481018e + 00 \text{ for } p = 4, \\ L &= 1.593715e + 00 \text{ for } p = 5, \end{aligned}$$

suggest $p = 2$ to be the best choice.

Finally, we observe the influence of the parameter γ by comparing parameter tuples $(2, 2, \gamma)$ for $N = 3$, $c = 8$ and $p = 2$. Here

$$\begin{aligned} L =& 1.284659e + 00 \text{ for } \gamma = 4, \\ L =& 1.212759e + 00 \text{ for } \gamma = 4.5, \\ L =& 1.135887e + 00 \text{ for } \gamma = 5, \\ L =& 1.200003e + 00 \text{ for } \gamma = 5.5, \\ L =& 1.216268e + 00 \text{ for } \gamma = 6 \end{aligned}$$

show the influence.

The natural filter of $(1, 1, 2)$, the one of $(2, 2, 5)$ and the shaped raised cosine filter of 8th order can be seen and compared in figure 3.

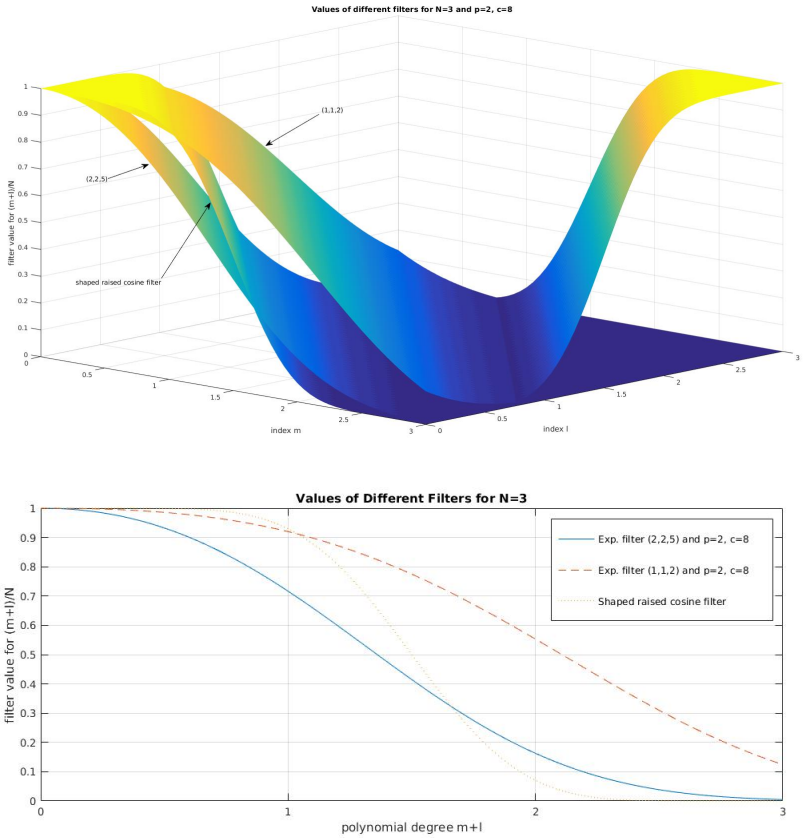
Values of different filters for N=3 and p=2, c=8
(1,1,2)
(2,2,5)
shaped raised cosine filter
filter value for (m+l)/N
index m
index l
Values of Different Filters for N=3
Exp. filter (2,2,5) and p=2, c=8
Exp. filter (1,1,2) and p=2, c=8
Shaped raised cosine filter
filter value for (m+l)/N
polynomial degree m+l

FIGURE 3. $(\alpha, \beta, \gamma) = (1, 1, 2)$, $(2, 2, 5)$ with their natural filters and the shaped raised cosine filter

We end this section by recommending the parameter tuple $(\alpha, \beta, \gamma) = (2, 2, 5)$ with $c = 8$ and filter order $p = 2$ for the polynomial degree $N = 3$. The following section will provide numerical test which build around this choices.

6. Numerical tests

After presenting our theoretical results we want to give a short numerical investigation to show that our conclusions are justified. We consider the two dimensional Burgers' equation

$$u_t(x,y,t) + u(x,y,t)\left(u_x(x,y,t) + u_y(x,y,t)\right) = 0$$

in the domain $[-1,1]^2$ with the initial condition

$$u_0(x,y) = \frac{1}{4} + \frac{1}{2}\sin\left(\pi(x+y)\right)$$

and periodic boundary conditions $u(-1,y,t) = u(1,y,t)$ and $u(x,-1,t) = u(x,1,t)$. At $t = 0.5s$ two discontinuities arise at $y = \frac{3}{2} - x$ and $y = \frac{5}{2} - x$. We use 1088 triangles for the spatial discretization and present the numerical solutions at $t = 0.45s$ for several parameter selections. Without filtering high oscillations already develop in much earlier calculations and the SD Method collapses.
In Tables 7-8 the minimum and maximum of the numerical solutions for filter parameters p and c are shown in the polynomial cases $(\alpha,\beta,\gamma) = (1,1,2)$ and $(2,2,5)$. These values give a first indication for the stability of the resulting method.

p	c	min	max
2	8	-3.24	6.00
3	8	-6.55	3.67
4	6	-12.32	6.03
4	8	-11.08	4.96

Table 7. $(\alpha,\beta,\gamma) = (1,1,2),\ t = 0.4s$

p	c	min	max
2	8	-1.55	2.46
3	8	-6.54	4.23
4	6	-3.10	5.98
4	8	-2.44	5.64

Table 8. $(\alpha,\beta,\gamma) = (2,2,5),\ t = 0.45s$

The polynomial degree N in these test-cases is always three. For most parameters p, c and (α,β,γ), we were not able to calculate in time further than $0.4s$. However, for the choice $p = 2$ and $c = 8$ motivated by our stability analysis we were indeed able to calculate till 0.45 for both parameters $(1,1,2)$ and $(2,2,5)$. In figure 4 the 2d and 3d plots of the numerical solutions are presented. No post-processing was applied.

Predicted by the stability analysis in section 5 and coinciding with tables 7 and 8, the selection of parameters $p = 2$ and $c = 8$ using the APK polynomials $(2,2,5)$ and their natural filters show significant stronger stability properties than for instance $(1,1,2)$. Here, two attributes play a key role in the calculation. First $(2,2,5)$ has a small condition number, see table 1. But second and quiet more important are the good properties - using the natural filter with $\gamma = 5$ - from point of *linear* stability, suggested by the stability analysis in section 5. Following this observation, we wish to combine a small condition number like for $(1,1,2)$ and the good stability of the choice $(\alpha,\beta,\gamma) = (2,2,5)$ with $p = 2$ and $c = 8$. Therefor we next observed the

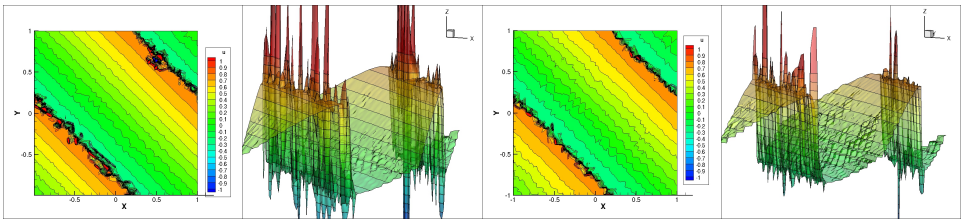

$(\alpha, \beta, \gamma) = (1, 1, 2),\ t = 0.45s$ $(\alpha, \beta, \gamma) = (2, 2, 5),\ t = 0.45s$

FIGURE 4. $N = 3$, $p = 2$, $C = 8$

polynomial basis of $(1, 1, 2)$, however equipped with the natural filter of $(2, 2, 5)$ instead of it's own one. I.e we choose $\gamma = 5$ in (4.9) instead of the natural choice $\gamma = 2$. The resulting numerical solutions, again presented in a 2d and 3d plot, can be seen in figure 5 and once more show an improvement.

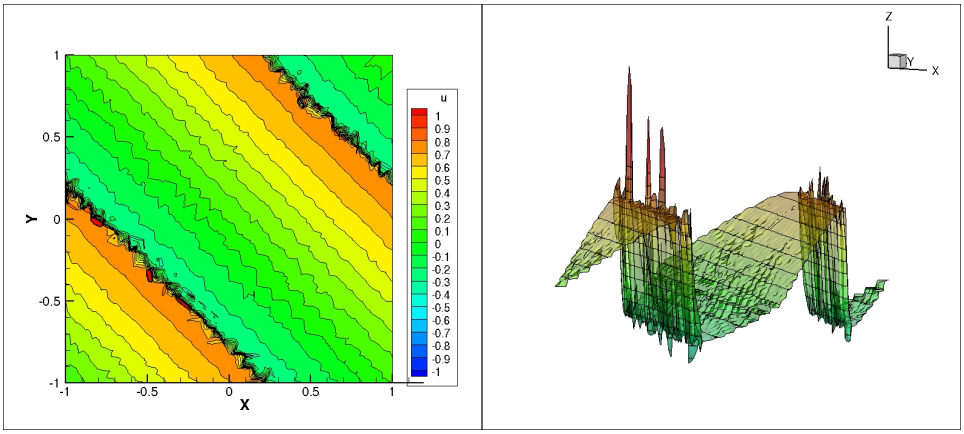

$t = 0.45s$ $t = 0.45s$

FIGURE 5. $(\alpha, \beta, \gamma) = (1, 1, 2)$ with the natural filter of $p = 2$, $c = 8$ and $(2, 2, 5)$

7. Discussion and Conclusion

We started this paper by extending the SD method by more general bases of APK polynomials instead of Lagrange or PKD polynomials and instantly observed their numerical qualification by their condition numbers. The classical SD method was known to be unstable on triangular elements and unfortunately we were able to obtain the same result for every extended version of the SD method. Hence addressing the problem of Gibb's phenomenon, which often leads unstable schemes to blow up, we applied the well known SV method to milder instabilities. Due to the APK polynomials to fulfill certain eigenvalue problems, we derived an equivalent but from point of computational costs much more efficient formulation of the SV method via modal filtering by natural exponential filters with respect to the polynomial basis. Whole new error estimates for filtered APK extensions for

smooth functions then were given. We also gave a von Neumann analysis for linear stability for the extended SD method with modal filtering by natural filters of APK polynomials. The idea was for the right choice of APK polynomials to may have some positive influence on the stability and accuracy of the method. To the best of our knowledge, this work was the first to give such an analysis for a scheme with spectral filtering. This stability analysis indeed suggested a certain choice of APK polynomials and parameters in their natural filters, which then were observed in a short numerical investigation. The numerical solutions we obtained show significant stronger stability properties than the ones resulting from classical SD methods. By combining our results from the analysis of condition numbers and linear stability for different APK polynomials, we equipped basis polynomials with favorable condition numbers with modal filters coming from a polynomial basis with strong stability properties. Once more, this led to a significant improvement of the numerical solutions.

Despite this, it should also be said that Flux Reconstruction (FR) or Correction Procedure via Reconstruction (CPR) methods nowadays are getting more more interesting, due to their strong stability properties, while SD methods are receiving decreasing attention. We still analyzed modal filtering based on SD methods to investigate the pure influence of the orthogonal polynomials and their natural filters. In the FR/CPR approach a correction term is applied which might cancel out effects of the filter. However, the observations made for spectral filtering in this paper target a first step to both a better understanding of the influence of spectral filtering and in future to gainfully adapt these ideas to FR/CPR methods. Improvements might be higher CFL numbers, thus larger time steps and more efficient methods, as well as more advanced methods in post-processing.

In future researches further developments for modal filtering itself would be favorable. Due to high condition numbers of the Vandermonde matrix for several bases of APK polynomials, we had to restrict ourself to certain subranges of parameter families. However, it could be possible to find filters with even better properties outside of these subranges. To bypass the problem of quite bad condition numbers in this new ranges, it would be promising to work with projection approaches in the series expansion, instead of interpolation ones.

8. Appendix:

$M_i^{m,n}$ for the SD Method of 3rd order ($K_s = 6, K_F = 10$):

$$
\begin{aligned}
M_1^{-1,0} &= \mathrm{diag}(E_{4\times4}, 0_{6\times6}),\\
M_1^{0,0} &= \mathrm{diag}(0_{5\times5}, E_{2\times2}, 0_{1\times1}, E_{2\times2}),\\
M_1^{0,-1} &= \mathrm{diag}(0_{4\times4}, E_{1\times1}, 0_{2\times2}, E_{1\times1}, 0_{2\times2}),\\
M_2^{-1,0} &= \mathrm{diag}(0_{1\times1}, E_{2\times2}, 0_{7\times7}),\\
M_2^{0,0} &= \mathrm{diag}(0_{3\times3}, E_{1\times1}, 0_{1\times1}, E_{2\times2}, 0_{1\times1}, E_{1\times1}, 0_{1\times1}),\\
M_2^{0,-1} &= \mathit{diag}(E_{1\times1}, 0_{3\times3}, E_{1\times1}, 0_{2\times2}, E_{1\times1}, 0_{1\times1}, E_{1\times1}).
\end{aligned}
$$

$M_i^{m,n}$ for the SD Method of 4th order ($K_s = 10, K_F = 15$):

$$
\begin{aligned}
M_1^{-1,0} &= \operatorname{diag}(E_{5\times 5}, 0_{10\times 10}),\\
M_1^{0,0} &= \operatorname{diag}(0_{6\times 6}, E_{3\times 3}, 0_{1\times 1}, E_{2\times 2}, 0_{1\times 1}, E_{2\times 2}),\\
M_1^{0,-1} &= \operatorname{diag}(0_{5\times 5}, E_{1\times 1}, 0_{3\times 3}, E_{1\times 1}, 0_{2\times 2}, E_{1\times 1}, 0_{2\times 2}),\\
M_2^{-1,0} &= \operatorname{diag}(0_{1\times 1}, E_{3\times 3}, 0_{11\times 11}),\\
M_2^{0,0} &= \operatorname{diag}(0_{4\times 4}, E_{1\times 1}, 0_{1\times 1}, E_{3\times 3}, 0_{1\times 1}, E_{2\times 2}, 0_{1\times 1}, E_{1\times 1}, 0_{1\times 1}),\\
M_2^{0,-1} &= diag(E_{1\times 1}, 0_{4\times 4}, E_{1\times 1}, 0_{3\times 3}, E_{1\times 1}, 0_{2\times 2}, E_{1\times 1}, 0_{1\times 1}, E_{1\times 1}).
\end{aligned}
$$

$M_i^{m,n}$ for the SD Method of 5th order ($K_s = 15, K_F = 21$):

$$
\begin{aligned}
M_1^{-1,0} &= \operatorname{diag}(E_{6\times 6}, 0_{15\times 15}),\\
M_1^{0,0} &= \operatorname{diag}(0_{7\times 7}, E_{4\times 4}, 0_{1\times 1}, E_{3\times 3}, 0_{1\times 1}, E_{2\times 2}, 0_{1\times 1}, E_{2\times 2}),\\
M_1^{0,-1} &= \operatorname{diag}(0_{6\times 6}, E_{1\times 1}, 0_{4\times 4}, E_{1\times 1}, 0_{3\times 3}, E_{1\times 1}, 0_{2\times 2}, E_{1\times 1}, 0_{2\times 2}),\\
M_2^{-1,0} &= \operatorname{diag}(0_{1\times 1}, E_{4\times 4}, 0_{16\times 16}),\\
M_2^{0,0} &= \operatorname{diag}(0_{5\times 5}, E_{1\times 1}, 0_{1\times 1}, E_{4\times 4}, 0_{1\times 1}, E_{3\times 3}, 0_{1\times 1}, E_{2\times 2}, 0_{1\times 1}, E_{1\times 1}, 0_{1\times 1}),\\
M_2^{0,-1} &= diag(E_{1\times 1}, 0_{5\times 5}, E_{1\times 1}, 0_{4\times 4}, E_{1\times 1}, 0_{3\times 3}, E_{1\times 1}, 0_{2\times 2}, E_{1\times 1}, 0_{1\times 1}, E_{1\times 1}).
\end{aligned}
$$

Acknowledgements.

References

1. Y Allaneau and Antony Jameson, *Connections between the filtered discontinuous Galerkin method and the flux reconstruction approach to high order discretizations*, Computer Methods in Applied Mechanics and Engineering **200** (2011), no. 49, 3628–3636.
2. Harold L Atkins and Chi-Wang Shu, *Quadrature-free implementation of discontinuous galerkin method for hyperbolic equations*, AIAA journal **36** (1998), no. 5, 775–782.
3. Garrett E Barter and David L Darmofal, *Shock capturing with higher-order, pde-based artificial viscosity*, AIAA paper **3823** (2007), 2007.
4. MG Blyth and C Pozrikidis, *A lobatto interpolation grid over the triangle*, IMA journal of applied mathematics **71** (2006), no. 1, 153–169.
5. Mark H Carpenter and Christopher A Kennedy, *Fourth-order 2n-storage runge-kutta schemes*, Nasa tm **109112** (1994), 871–885.
6. Moshe Dubiner, *Spectral methods on triangles and other domains*, Journal of Scientific Computing **6** (1991), no. 4, 345–390.
7. Charles F Dunkl and Yuan Xu, *Orthogonal polynomials of several variables*, no. 155, Cambridge University Press, 2014.
8. Anne Gelb and Jared Tanner, *Robust reprojection methods for the resolution of the gibbs phenomenon*, Applied and Computational Harmonic Analysis **20** (2006), no. 1, 3–25.
9. David Gottlieb and Jan S Hesthaven, *Spectral methods for hyperbolic problems*, Journal of Computational and Applied Mathematics **128** (2001), no. 1, 83–131.
10. David Gottlieb and Steven A Orszag, *Numerical analysis of spectral methods: theory and applications*, vol. 26, Siam, 1977.
11. David Gottlieb and Chi-Wang Shu, *On the gibbs phenomenon and its resolution*, SIAM review **39** (1997), no. 4, 644–668.
12. Uffe Haagerup and Henrik Schlichtkrull, *Inequalities for jacobi polynomials*, The Ramanujan Journal **33** (2014), no. 2, 227–246.
13. Jan Hesthaven and Robert Kirby, *Filtering in legendre spectral methods*, Mathematics of Computation **77** (2008), no. 263, 1425–1452.
14. PG Huang, ZJ Wang, and Y Liu, *An implicit space-time spectral difference method for discontinuity capturing using adaptive polynomials*, AIAA paper **5255** (2005), 2005.

15. HT Huynh, *A flux reconstruction approach to high-order schemes including discontinuous Galerkin methods*, AIAA paper **4079** (2007), 2007.
16. ———, *High-order methods including discontinuous Galerkin by reconstructions on triangular meshes*, AIAA Paper **44** (2011), 2011.
17. HT Huynh, Zhi J Wang, and Peter E Vincent, *High-order methods for computational fluid dynamics: A brief review of compact differential formulations on unstructured grids*, Computers & Fluids **98** (2014), 209–220.
18. Antony Jameson, *A proof of the stability of the spectral difference method for all orders of accuracy*, Journal of Scientific Computing **45** (2010), no. 1-3, 348–358.
19. George Karniadakis and Spencer Sherwin, *Spectral/hp element methods for computational fluid dynamics*, Oxford University Press, 2013.
20. Robert M Kirby and Spencer J Sherwin, *Aliasing errors due to quadratic nonlinearities on triangular spectral/hp element discretisations*, Journal of engineering mathematics **56** (2006), no. 3, 273–288.
21. Tom Koornwinder, *Two-variable analogues of the classical orthogonal polynomials*, Theory and applications of special functions (1975), 435–495.
22. David A Kopriva, *A conservative staggered-grid chebyshev multidomain method for compressible flows. ii. a semi-structured method*, Journal of computational physics **128** (1996), no. 2, 475–488.
23. David A Kopriva and John H Kolias, *A conservative staggered-grid chebyshev multidomain method for compressible flow.*, Tech. report, DTIC Document, 1995.
24. Yen Liu, Marcel Vinokur, and ZJ Wang, *Spectral difference method for unstructured grids i: basic formulation*, Journal of Computational Physics **216** (2006), no. 2, 780–801.
25. Heping Ma, *Chebyshev–legendre spectral viscosity method for nonlinear conservation laws*, SIAM Journal on Numerical Analysis **35** (1998), no. 3, 869–892.
26. Yvon Maday, Sidi M Ould Kaber, and Eitan Tadmor, *Legendre pseudospectral viscosity method for nonlinear conservation laws*, SIAM Journal on Numerical Analysis **30** (1993), no. 2, 321–342.
27. Georg May and Antony Jameson, *A spectral difference method for the euler and navier-stokes equations on unstructured meshes*, AIAA paper **304** (2006), 2006.
28. Andreas Meister, Sigrun Ortleb, and Thomas Sonar, *Application of spectral filtering to discontinuous galerkin methods on triangulations*, Numerical Methods for Partial Differential Equations **28** (2012), no. 6, 1840–1868.
29. Andreas Meister, Sigrun Ortleb, Thomas Sonar, and Martina Wirz, *An extended discontinuous galerkin and spectral difference method with modal filtering*, ZAMM-Journal of Applied Mathematics and Mechanics/Zeitschrift für Angewandte Mathematik und Mechanik **93** (2013), no. 6-7, 459–464.
30. Philipp Öffner, *Zweidimensionale klassische und diskrete orthogonale polynome und ihre anwendung auf spektrale methoden zur lösung von hyperbolischen erhaltungsgleichungen*, Braunschweig University, 2015.
31. Philipp Öffner and Thomas Sonar, *Spectral convergence for orthogonal polynomials on triangles*, Numerische Mathematik **124** (2013), no. 4, 701–721.
32. Philipp Öffner, Thomas Sonar, and Martina Wirz, *Detecting strength and location of jump discontinuities in numerical data*, Applied Mathematics **4** (2013), no. 12, 1.
33. Sigrun Ortleb, *Ein diskontinuierliches galerkin-verfahren hoher ordnung auf dreiecksgittern mit modaler filterung zur lösung hyperbolischer erhaltungsgleichungen*, kassel university press GmbH, 2011.
34. Per-Olof Persson and Jaime Peraire, *Sub-cell shock capturing for discontinuous galerkin methods*, AIAA paper **112** (2006), 2006.
35. Hendrik Ranocha, Philipp Öffner, and Thomas Sonar, *Summation-by-parts operators for correction procedure via reconstruction*, Journal of Computational Physics **311** (2016), 299–328.
36. Pavel Kondrat'evič Suetin, *Orthogonal polynomials in two variables*, vol. 3, CRC Press, 1999.
37. Yuzhi Sun, Zhi Jian Wang, and Yen Liu, *High-order multidomain spectral difference method for the navier-stokes equations on unstructured hexahedral grids*, Communications in Computational Physics **2** (2007), no. 2, 310–333.
38. Eitan Tadmor, *Convergence of spectral methods for nonlinear conservation laws*, SIAM Journal on Numerical Analysis **26** (1989), no. 1, 30–44.

39. Kris Van den Abeele, Chris Lacor, and Zhi Jian Wang, *On the connection between the spectral volume and the spectral difference method*, Journal of Computational Physics **227** (2007), no. 2, 877–885.
40. Kris Van den Abeele, Chris Lacor, and ZJ Wang, *On the stability and accuracy of the spectral difference method*, Journal of Scientific Computing **37** (2008), no. 2, 162–188.
41. Hervé Vandeven, *Family of spectral filters for discontinuous problems*, Journal of Scientific Computing **6** (1991), no. 2, 159–192.
42. Peter E Vincent, Patrice Castonguay, and Antony Jameson, *Insights from von Neumann analysis of high-order flux reconstruction schemes*, Journal of Computational Physics **230** (2011), no. 22, 8134–8154.
43. ———, *A new class of high-order energy stable flux reconstruction schemes*, Journal of Scientific Computing **47** (2011), no. 1, 50–72.
44. ZJ Wang, *High-order methods for the euler and navier–stokes equations on unstructured grids*, Progress in Aerospace Sciences **43** (2007), no. 1, 1–41.
45. ZJ Wang and Haiyang Gao, *A unifying lifting collocation penalty formulation including the discontinuous Galerkin, spectral volume/difference methods for conservation laws on mixed grids*, Journal of Computational Physics **228** (2009), no. 21, 8161–8186.
46. ZJ Wang, Yen Liu, Georg May, and Antony Jameson, *Spectral difference method for unstructured grids ii: extension to the euler equations*, Journal of Scientific Computing **32** (2007), no. 1, 45–71.
47. Martina Wirz, *Ein spektrale-differenzen-verfahren mit modaler filterung und zweidimensionaler kantendetektierung mithilfe konjugierter fourierreihen*, Cuvillier, 2012.
48. ———, *Detecting edges in high order methods for hyperbolic conservation laws*, High Order Nonlinear Numerical Schemes for Evolutionary PDEs, Springer, 2014, pp. 151–167.
49. Meilin Yu, ZJ Wang, and Yen Liu, *On the accuracy and efficiency of discontinuous galerkin, spectral difference and correction procedure via reconstruction methods*, Journal of Computational Physics **259** (2014), 70–95.

Technische Universität Braunschweig, Institut Computational Mathematics, Pockelsstrasse 14, D-38106 Braunschweig, Germany
E-mail address: j.glaubitz@tu-bs.de

Technische Universität Braunschweig, Institut Computational Mathematics, Pockelsstrasse 14, D-38106 Braunschweig, Germany
E-mail address: p.oeffner@tu-bs.de

Technische Universität Braunschweig, Institut Computational Mathematics, Pockelsstrasse 14, D-38106 Braunschweig, Germany
E-mail address: t.sonar@tu-bs.de